5-2017

Provenance Tracing of Glacial Sediment from the Foundation, Academy, and Recovery Ice Streams, Weddell Sea, Antarctica

Ashley Marie Cirone

Abstract

This project seeks to advance our understanding of Antarctic Ice Sheet dynamics and to gain insight into the bedrock composition beneath the Antarctic Ice Sheet by "fingerprinting" ice streams that drain into the Ronne-Filchner Ice Shelf. The Ronne-Filchner Ice Shelf is the second largest ice shelf in Antarctica and receives ice drained from both the West and East Antarctic Ice Sheets through a series of ice streams. In response to global warming, this sector has the potential to contribute dramatically to sea level rise, especially from the Recovery Catchment. Till samples were collected from lateral moraines adjacent to the Foundation, Academy, and Recovery ice streams, all located within the Weddell Sea sector, during a December 2014 field season. Extensive analyses of sieved fine fraction (< 63 μm) show that all three ice streams have major element profiles that are consistent with the upper continental crust, though with Na and Ca depletion. Al/Ti and Fe/Ti ratios are also consistent with upper continental crust for all three ice streams. Recovery Ice Stream is the only one of the three ice streams to contain Mn- bearing minerals, including psilomelane and hausmannite. Foundation Ice Stream is the only stream containing V- bearing titanomagnetite. The Foundation Ice Stream also contains the most ilmenite. Academy Glacier till exhibits the most alteration textures in Fe-oxides (63%), and Recovery exhibits the most homogeneous Fe-oxide grains (24%). Through developing these geochemical and mineral signatures, this project will allow researchers to develop proxy records for ice stream activity in marine sedimentary records and better understand which ice streams may be the most vulnerable to ice loss as a response to global warming.

MONTCLAIR STATE UNIVERSITY

Provenance Tracing of Glacial Sediment from the Foundation, Academy, and Recovery Ice Streams, Weddell Sea, Antarctica

by

Ashley Marie Cirone

A Master's Thesis Submitted to the Faculty of

Montclair State University

In Partial Fulfillment of the Requirements

for the Degree of

Master of Science

May 2017

College of Science and Mathematics

Department of Earth and Environmental Studies

Thesis Committee:

[redacted]

Dr. Stefanie Brachfeld
Thesis Sponsor

[redacted]

Dr. Matthew L. Gorring
Committee Member

[redacted]

Dr. Sandra Passchier
Committee Member

Provenance Tracing of Glacial Sediment from the Foundation, Academy, and Recovery Ice Streams, Weddell Sea, Antarctica

A THESIS

Submitted in partial fulfillment of the requirements

for the degree of Master of Science

by

Ashley Marie Cirone

Montclair State University

Montclair, NJ

May 2017

Acknowledgments

I would first like to thank my thesis advisor, Dr. Stefanie Brachfeld for this incredible opportunity as well as for all her time and support. She always had an open office and a helpful hand whenever I ran into any trouble or needed a push in the right direction. I would also like to thank Dr. Xiaona Li for assistance with ICP-MS analyses and Dr. Laying Wu for guidance with the SEM. A very special thank you to Dr. Kathy Licht, Dr. Trevor Williams, and Dr. Sidney Hemming for providing samples, field notes, and helpful discussions and advice along the way. Also thank you to the National Science Foundation Office of Polar Program grant 1342000 and Major Research Instrumentation grant 1531719.

Special thanks go to all of the people who have supported me implicitly over the last two years; Jennifer Light and April Kelly for their suggestions, all of the much needed coffee runs and many adventures along the way; Marissa Teator and Emma Hogan keeping me on my toes, in shape, and always relaxed when home; Dr. Jacqueline Smith with copious amounts of advice and pushing me as an undergraduate to pursue this degree; and James Hodge with wonderful words of encouragement, fantastic music, and amusing videos to help me get through the most stressful of days (not to mention allowing me to commandeer his desktop for hours on end).

An extraordinary thank you goes to my parents Anthony and Andrea Cirone. They have always taught me to be the best I can be and to never give up. Without their perpetual love and support I would not be where I am today.

Table of Contents

List of Figures

List of Tables

1. Introduction

The Ronne-Filchner Ice Shelf is the second largest ice shelf in Antarctica and receives ice drained from both the West and East Antarctic Ice Sheets (WAIS and EAIS, respectively) through a series of ice streams (Fig.1, Rignot et al., 2011). In response to global warming, the Weddell Sea Sector has the potential to contribute dramatically to sea level rise as 22% of all Antarctic ice drains through this sector (Bamber et al., 2007; Hillenbrand et al., 2014). A recent study suggests that the Recovery Catchment will be the source for the majority of future ice loss from East Antarctica (Golledge, et al., 2017). Recovery Catchment is one of several drainages within the EAIS and WAIS that are vulnerable to ocean warming and undermelting of ice as warm Circumpolar Deep Water (CDW) moves landward within subglacial troughs (Golledge et al., 2017). It is uncertain how fast ice streams might transfer ice from land to ocean due to warming air and ocean temperatures (Thomas et al., 2015; Golledge et al., 2017). Records of past ice sheet movement are preserved within marine sediment cores, and this can help in potentially answering these questions (Hillenbrand et al., 2014) as well as providing input data for modeling future ice sheet loss and sea level rise.

This project seeks to advance our understanding of Antarctic Ice Sheet dynamics and to gain further insight into the bedrock composition beneath the Antarctic Ice Sheet through geochemical and mineral "fingerprinting." The fingerprinting of ice streams involves creating a suite of tracers for terrestrial glacial debris that can be used to correlate ice rafted debris in marine sedimentary records to the drainage basin from which it was eroded. There are many different provenance tracers used, such as lithic assemblages within the sand fraction (Licht et al., 2005), bulk sediment geochemistry

(Farmer et al., 2006), Ar/Ar dating of hornblende grains and radioisotope geochemistry (Roy et al., 2007; Williams et al 2010; Pierce et al., 2014), U/Pb dating of zircons (Košler et al., 2002), heavy mineral assemblages (Passchier, 2007), clay mineral assemblages (Biscaye, 1965; Hillenbrand et al., 2014), and Fe-oxide assemblages (Darby and Bischof, 1996, 2001). Through the development of these types of signatures for Weddell Sea Sector ice streams, this project will allow researchers the ability to develop and improve proxy records for ice stream activity in marine sediment records. These results will provide insight to the felsic or mafic nature of bedrock under each ice stream and how enriched or depleted each ice stream is with respect to different elements of interest as compared with average continental crust.

In addition to identifying provenance signatures, quantifying elemental abundances from potential source regions will be useful in interpreting geochemical proxies of paleoproductivity and paleoredox conditions in Weddell Sea sector marine sediment cores. Fe is a micronutrient that can stimulate phytoplankton blooms, which consume dissolved CO_2 from the surface ocean, resulting in CO_2 drawdown from the atmosphere. Increased productivity has been observed in the Weddell Sea surrounding large icebergs, which is caused by input of Fe and other micronutrients as the icebergs melt (Smith et al., 2007; Duprat et al., 2016). Therefore, the potential for glacial debris to supply bioavailable Fe to the ocean is of interest. Enrichment of redox-sensitive elements such as V and Mn in sediment cores can be used to monitor changes in bottom water oxygen levels, which is of interest in the Weddell Sector since this is an area of Antarctic Bottom Water formation (Orsi et al., 1999). This study will explore how much Fe may be supplied to the Weddell Sea embayment by the Foundation, Academy, and Recovery Ice

Streams. The results are reported as total Fe, as quantifying bioavailable Fe is beyond the scope of this thesis. In addition, we report the detrital abundances of metals used as tracers of redox conditions in sediment such as V and Mn. Determining baseline values of detrital V and Mn will be an asset to evaluating whether detrital input can obscure patterns of enrichments or depletions due to redox processes in marine sediment cores (Haug et al., 2001; Yarincik et al., 2000; Latimer et al., 2006).

Of the many ice streams within the Weddell Sea Sector, we examined three major ice streams that discharge significant amounts of ice to the Weddell Sea. The Foundation, Academy, and Recovery Ice Streams lie within the two largest ice drainages in Antarctica. The Recovery Ice Stream lies within East Antarctica, while the Foundation Ice Stream and Academy Glacier entrain sediment from both East and West Antarctica (Fig.1, Rignot et al., 2011). Till samples were collected from lateral moraines adjacent to each ice stream during a December 2014 field season. The till was used to develop a comprehensive suite of tracers in collaboration with colleagues at Texas A&M University, Lamont Doherty Earth Observatory, Cambridge University, UK, and the Alfred Wegener Institute, Germany (Agrios et al. 2016; Cirone et al., 2016; Williams et al., 2016).

This study focuses on bulk sediment geochemistry of the < 63 μm sediment size fraction (the mud fraction) and the texture and composition of course silt to medium sand-sized iron oxide grains. Fe oxide mineral grains have distinctive textures and compositions, lack cleavage, and have moderately high hardness (5.5 to 6.5 on the Mohs hardness scale), making them excellent provenance tracers. The grains can be differentiated into several distinct compositional categories for each source area and can

be clustered into subgroups depending upon the host mineral and the presence and abundance of trace elements that substitute for Fe and Ti (i.e. Mg, Al, V, Cr, and Mn). Darby and Bischof, (1996 and 2001), and Darby (2015) used this technique in the Arctic Ocean to match ice rafted debris (IRD) recovered in sediment cores to terrestrial sources, allowing the authors to make inferences regarding ice sheet dynamics and the circulation of sea ice in the Arctic Ocean.

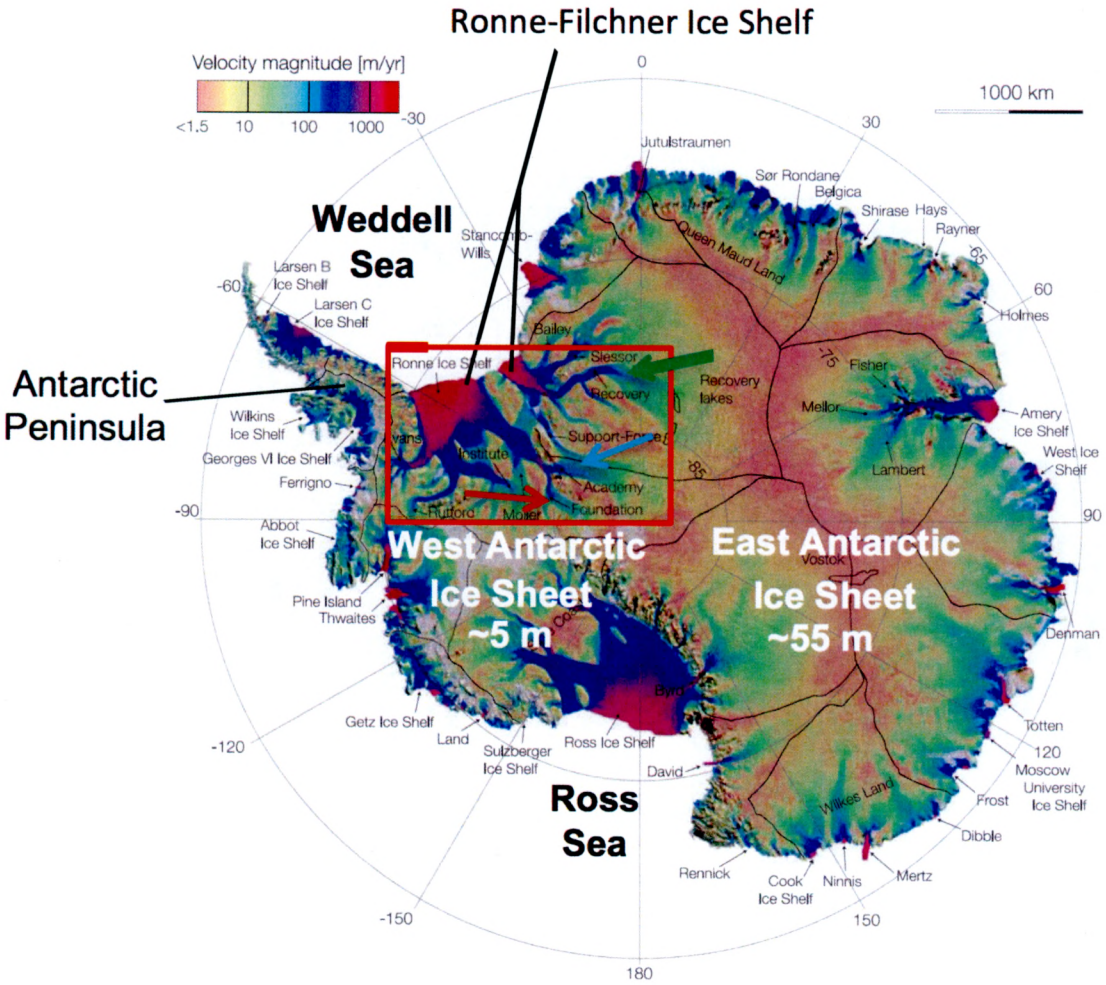

Figure 1. Antarctic ice drainages and ice flow velocity map of Rignot et al., 2011. The red box denotes the location of the Foundation (red arrow), Academy (blue arrow), and Recovery (green arrow) Ice Streams in the Weddell Sea sector. The West Antarctic Ice Sheet has the potential to add approximately 5 meters to sea level rise while the East Antarctic Ice Sheet will potentially add approximately 55 meters to sea level rise. (Image adapted from Rignot et al., 2011).

2. Study Area

The Recovery Glacier and Ice Stream system (hereafter referred to as Recovery Ice Stream) lies within East Antarctica immediately south of the Shackleton Range, and flows southeast to northwest (Fig. 2). The ice thickness estimated from BEDMAP2 (Fretwell et al., 2013) varies from approximately > 3000 m at its head to < 1000 m as it approaches the Filchner Ice Shelf. The BEDMAP2 ice thickness map suggests that Foundation Ice Stream and Academy Glacier are thinner, with maximum ice thickness < 2500 m.

Low-grade (greenschist facies) metasedimentary and metavolcanic rocks comprise the Shackleton Range, which is inferred to have been uplifted during the Ross Orogeny (500 - 444 Ma). The Shackleton Range may also include medium grade metamorphic rocks formed during one or more Precambrian events (Craddock, 1970). During the 2014 field season, the field team observed multiple lithologies from cobbles and boulders at the Recovery Ice Stream site, which consisted of limestones, Ferrar dolerite, schist, and quartzite (Williams et al., 2015, 2016).

The Academy Glacier and Foundation Ice Stream may entrain debris from both East and West Antarctica (Fig. 2). Academy Glacier flows southeast to northwest, between the Patuxent and Neptune ranges (Fig. 3), and then merges with the Foundation Ice Stream. The Foundation Ice Stream is approximately 240 km long and flows south to north along the western margin of the Pensacola Mountains (Stewart, 1952; Fig. 3). The Pensacola Mountains were uplifted during the Ellsworth Orogeny, during the late Triassic to early Jurassic between 237 and 174 Ma. The range is predominantly composed of low-

grade metasedimentary and metavolcanic rocks (mainly greenschist; Fig. 3). The northern end of the Foundation Ice Stream lies within the Dufek Massif, a range of exposed peaks in the Pensacola Mountains. The massif is home to the Dufek intrusion, estimated to be Jurassic in age, consisting of Ferrar Group of basalts and diabases that are found throughout the Transantarctic Mountains. The Dufek Massif also includes well-layered, magnetite-bearing pyroxene gabbros as well as Ca-poor pyroxenes (Ford, 1976). Sections of the Pensacola Mountains also contain granite emplaced during the Ross and Ellsworth orogenies. Moving inland, the range turns into a similar lithofacies as the Shackleton Range - Ross Orogen low-grade metasedimentary and metavolcanic rocks - then transitions into sedimentary rocks of the Gondwana sequence (Craddock, 1970). This belt of Gondwana sequence rocks extends from Coats Land along the eastern Weddell Sea margin all the way to western Wilkes Land coast in East Antarctica (Craddock, 1970).

The only exposed outcrop in the area visited during the 2014 field season is located in the Thomas Hills. The bedrock located here is a part of the Patuxent Formation, late Precambrian in age, and composed of meta-subgraywake and slate mixed with basaltic and felsic volcanic material (Ford et al., 1978). Cobble and boulder lithologies observed in till next to the Academy Glacier include white granite, purple-red sandstone, volcanics, and lithologies interpreted as turbidites from the Patuxent Formation (Williams et al., 2015, 2016). Lithologies observed at the Foundation Ice Stream sites include Patuxent turbidites, sandstones that are red, yellow, and white in color, conglomerates, mafic igneous rocks, greenish granitic boulders, and black, gray, and white limestones (Williams et al., 2015).

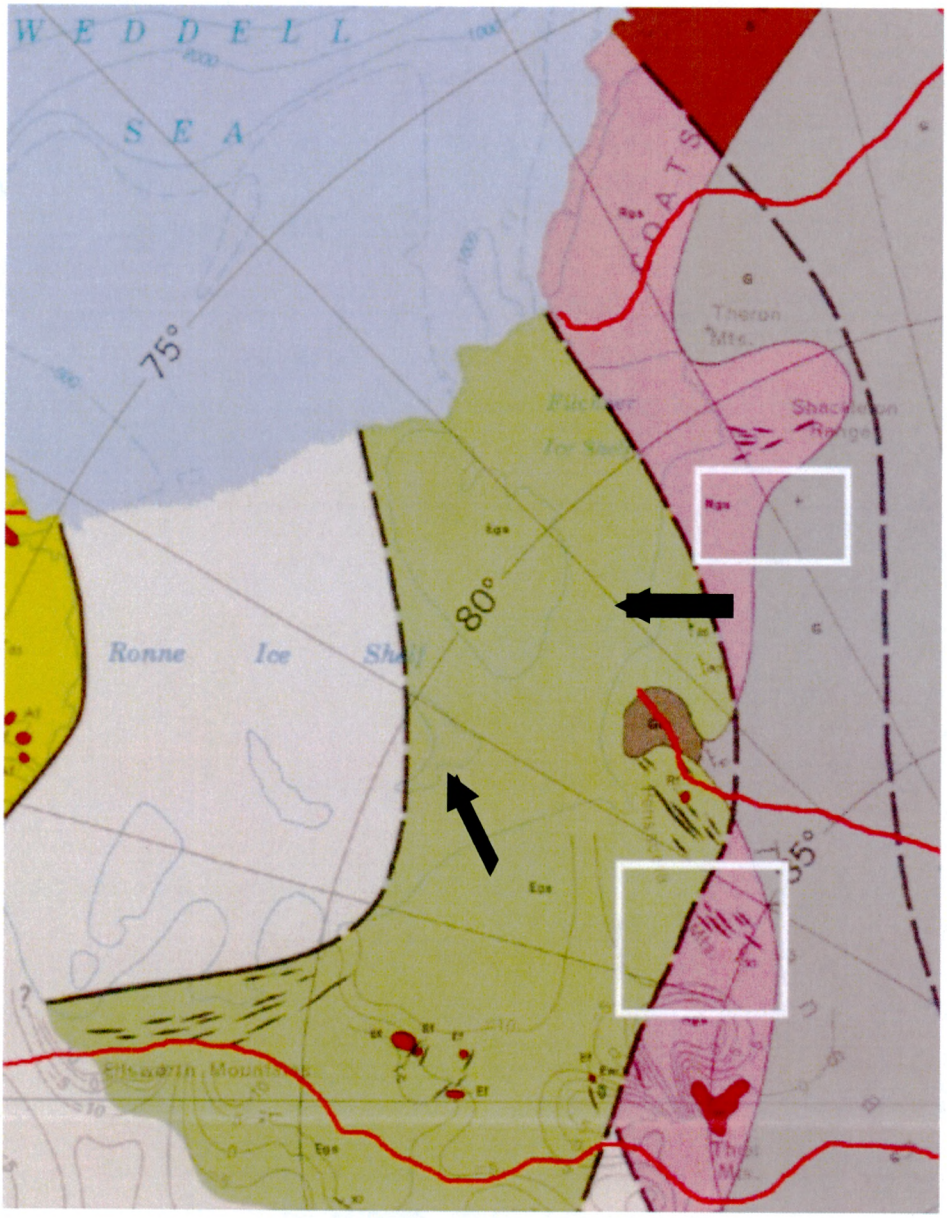

Figure 2. Tectonic map of the Weddell Sea Sector; white boxes denote locations of Recovery Ice Stream (upper box, directly south of the Shackleton Range), the Academy Glacier (running through the Pensacola Mountains) and Foundation Ice Stream (immediately west of the Pensacola Mountains). Light green represents low-grade meta-sedimentary and meta-volcanic rocks (237-174 Ma). Pink represents meta-sedimentary and meta-volcanic rocks (500-444 Ma). Grey represents Gondwana sequence sedimentary rocks. Solid red lines represent drainage basins and arrows indicate direction of ice flow (image adapted from Craddock, 1970).

Figure 3. Geologic map of the Pensacola Mountains adjacent to the Academy Glacier and Foundation Ice Stream. Solid grey represents Patuxent Formation grey-green argillaceous sandstones and slate. Grey with blue horizontal lines represents grey basalt interlayered with Patuxent sandstones. Light pink represents Neptune Group sandstones that are Ordovician in age (Schmidt and Ford, 1969).

3. Methods

3.1. Study Area and Field Methods

Twenty-one onshore surface till samples were collected from moraines adjacent to three ice streams that were accessible by aircraft and/or skidoos during a December 2014 field season, at distances of approximately 87.5 to 150 km from the inferred grounding line position (Table 1; Fig. 4). Square-meter plots were mapped out with rope (Fig. 5). Pebbles and cobbles were picked from the surface for lithologic identification. To avoid the possibility that wind scouring biased the grain size distribution and composition of the surface sediment, approximately 1 cm was removed from the surface of the plots prior to sampling. Approximately 2 kg of unconsolidated sediment was scooped from a depth of 2 to 5 cm into plastic bags, which were then mixed and homogenized, then subdivided into subsamples for each investigator.

Table 1. Sample site locations, identification codes, and associated ice streams

Sample Site	Sample ID	Ice Stream	Latitude (S)	Longitude (W)
Mt. Yarborough	YAR-2	Foundation	-84.4198	-65.8992
Mt. Yarborough	YAR-3	Foundation	-84.409	-65.9705
South Island	SIS-1	Foundation	-84.4418	-66.2704
South Island	SIS-2	Foundation	-84.4459	-66.2323
Mt. Suyden	SUY-1	Foundation	-84.5326	-65.4768
Hemming Nunatak	HEM-1	Foundation	-84.4401	-65.3698
Moustache Moraine	MOU-1	Foundation	-84.3303	-65.0988
Moustache Moraine	MOU-2	Foundation	-84.3304	-65.0983
Mt. Yarborough moraine	YAR-4a	Foundation	-84.4296	-66.0726
Mt. Yarborough moraine	YAR-4b	Foundation	-84.4195	-66.072
Mt. Yarborough moraine	YAR-4c	Foundation	-84.4192	-66.0604
Martin Peak	MAR	Foundation	-84.3674	-65.3049
Martin Peak moraine	MAM PEBTIL	Foundation	-84.3521	-65.2362
Martin Peak moraine	MAM2 PEBTIL	Foundation	-84.3534	-65.2459
Weber Ridge	WEB PEBTIL	Academy	-84.295	-62.8646
N. Side Academy Glacier	LIC PEBTIL	Academy	-83.9007	-57.4212
N. Side Academy Glacier	LIC2 PEBTIL	Academy	-83.8981	-57.4246
Stephenson Bastion moraine	STB PEBTIL	Recovery	-80.8047	-27.2401
Stephenson Bastion moraine	STB2 PEBTIL	Recovery	-80.8046	-27.2398
Whichaway Nunataks moraine	WAW PEBTIL	Recovery	-81.5058	-28.6816
Whichaway Nunataks moraine	WAW2 PEBTIL	Recovery	-81.5063	-28.6858

PEBTIL = Pebble Till

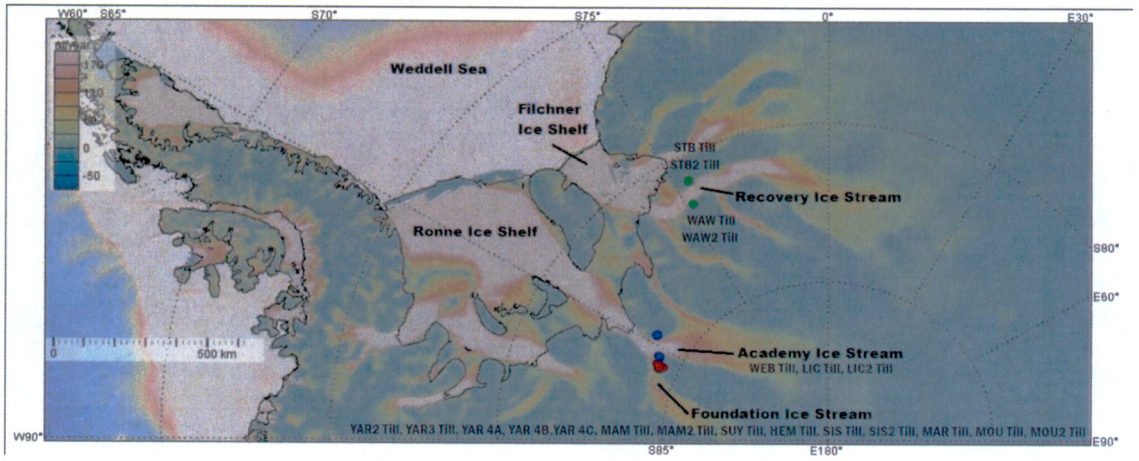

Figure 4. Locations of till sample collection sites. Green dots signify Recovery Ice Stream sample sites, blue dots signify Academy Glacier sites, and the red dots signify Foundation Ice Stream sites (image generated using GeoMapApp). The "Antarctic Coastline" overlay in GeoMapApp (solid black line) is the combination of the coastline, ice shelf edges, and inferred grounding line locations from Fretwell et al., 2013. The sample sites are approximately 87.5 to 150 km upstream of the grounding line.

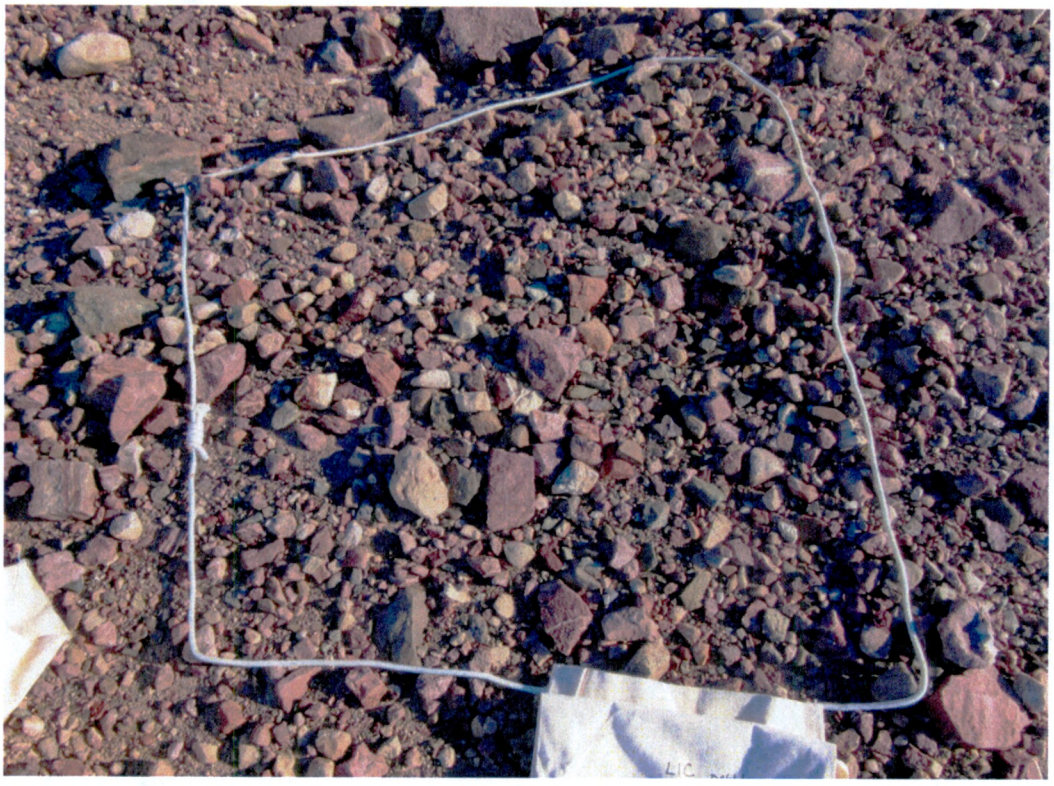

Figure 5. Example of $1m^2$ plot of till at the LIC field site adjacent to the Academy Glacier (photograph courtesy of Kathy Licht).

3.2. Initial Sample Processing

The twenty-one sediment samples were processed via two sieving steps and by magnetic separation for chemical and mineral analysis. Each bulk sediment sample was weighed out twice to approximately 15 grams and deposited into pre-labeled glass beakers. Labels contained the collection site name, date of collection, and size fraction. One bulk sample of 15 grams was sieved into 45-500 μm and 500-2000 μm size fractions, and the other was sieved into < 63 μm and > 63 μm size fractions. The 45-500-2000 μm beaker was filled with 50 mL of Calgon solution to disaggregate the sediment. The < 63μm beaker used only nanopure water to preclude cations absorbing onto clay particles and altering the chemistry of the sample.

After sonicating the samples were wet sieved. The 45-500 μm and 500-2000 μm size fractions were oven dried at 45 °C. The 45-500 μm size fraction was used for iron oxide extraction, which is described in section 3.4.1. The 500-2000 μm size fraction was not used in this study, but is archived for any future grain mounts and point counting, following the method of Licht et al. (2005).

The < 63 μm sample was poured into pre-labeled centrifuge tubes and centrifuged at 3500 rpm for fifteen minutes or until there was visible separation between sample and water and the water was completely clear and colorless; the clear water was pipetted out. Samples were then frozen at -20 °C for at least 24 hours, and then freeze-dried for 24-36 hours using a Labconco Freezone freeze-dryer in order to dry the sample prior to geochemical analysis and future magnetic analysis of the fine fraction. The freeze-dried sample was then used for geochemical analysis described in section 3.3.

3.3. Major and Trace Element Geochemistry via ICP-OES and ICP-MS

3.3.1 Sample fusion

Sediment samples were prepared for inductively coupled plasma optical emission spectrometry (ICP-OES) and mass spectrometry (ICP-MS) by starting with lithium-metaborate fusion. Subsamples from the < 63 μm size fraction were weighed out to 0.1000 ± .0005 g and thoroughly mixed with 0.4000 ± 0.020 g of lithium metaborate flux. Once mixed, the samples were carefully poured into graphite crucibles. The crucibles were placed in a muffle furnace at 1050 °C for approximately 25 minutes, which created a glass bead that dissolves easily in nitric acid. After removal from the furnace, the bead was transferred to a Savillex beaker containing 50 mL of 7% nitric acid. Beakers were set on stirring plates to allow the stir rods to expedite the dissolution process. After the samples were completely dissolved, the solution was filtered into 60 mL Nalgene bottles, resulting in a 500x dilution of the sample. Each set of 6-8 samples was prepared along with one blank containing only the lithium metaborate flux.

3.3.2 Sample Dilution for ICP-OES and ICP-MS

For analysis via the ICP-OES, solutions were diluted to 4000x using 2% nitric acid. Approximately 6.5 mL of each 500x sample was pipetted into a new 60 mL Nalgene bottle and mixed with 50 mL of the 2% nitric acid. Samples were stored in a refrigerator until analysis. In total, 41 samples, including till samples, US Geological Survey powdered reference materials standards, and blanks, were prepared for analysis.

The ICP-MS requires a 10,000x dilution. Using the previously prepared 500x samples, blanks, and standards, 0.5 mL of sample was pipetted into a clean test tube and

mixed with 9.5 mL of 1% nitric acid. Dilutions were made either immediately prior to analysis, or no more than 1 day prior to analysis.

3.3.3 Sample Analysis and Data processing

Major elements were analyzed on a JY Horiba ICP-OES at Montclair State University using the 4000x dilution. Trace elements were analyzed on a ThermoFisher iCAP ICP-MS using the 10,000x dilution. Every run contained samples, blanks, and standards. Each individual analysis consisted of three replicate measurements of the solution. A drift solution was measured after every 4 samples to monitor instrument drift and correct data for changes in instrument operating conditions. Raw output was drift-corrected, blank corrected, and then calibrated to units of wt% or ppm using a calibration line derived from standards.

Ten primary and 2 secondary U.S. Geological Survey Powdered Geochemical Reference Materials were prepared using the same procedure as described above. The 10 primary standards (all igneous materials) were used to derive a calibration line for each element of interest. This was done using Microsoft Excel's line fit function. Three runs were conducted on each instrument. Each individual run was corrected and calibrated. Finally, the average wt% or average ppm for each element and standard deviation of the 3 runs was calculated for each sample. The two secondary standards, both sedimentary materials, were used to check the accuracy of the calibration.

3.4 Scanning Electron Microscopy and X-ray Microanalysis

3.4.1 Fe-Oxide Sample Preparation

The 45-500 μm fraction was passed through a Frantz Magnetic Separator set to downhill and side slopes of 25 degrees and 0.4 amps of electrical current. Two vessels were attached to the end of the device in order to catch the magnetic and the non-magnetic fractions as the sediment passed through the magnetic field. The magnetic fraction was examined under a stereomicroscope and hand-picked for opaque grains with metallic luster. These grains were then mounted in epoxy within a Lucite disk (hereafter referred to as grain mounts), with each sample occupying a separate 0.125" drill hole within the disk.

Grain mounts were ground and polished beginning with the coarsest grinding of 600 SiC for five minutes. Disks were then polished for one hour using 6 μm diamond polishing solution, followed by one hour using 1 μm diamond polishing solution. Grain mounts were checked periodically during polishing to ensure that scratches and blemishes were being removed. All polished grain mounts were imaged using a Zeiss reflected light microscope in order to create a map of each set of grains and assign identification numbers to all potential iron-oxides that could be used for analysis. Grain mounts were then carbon coated using a Denton Desk IV Turbo Sputter Coater.

3.4.2 SEM Imaging and X-ray Microanalysis

Under low-magnification backscatter (BSE) imaging, a BSE map and an x-ray map were created to identify oxides vs. silicates. The x-ray maps were color-coded for ease of interpretation, with Fe colored red, Ti colored blue, and Si colored yellow. Grains

with resulting red, purple, and blue colors were determined to be Fe-oxides and were assigned identification numbers. Grains colored yellow were interpreted to be silicates and were not included in further analysis (Fig. 6). Close-up BSE images were taken of each numbered Fe-oxide grain for texture identification and to identify analytical regions for Energy Dispersive X-ray Spectrometry (EDS). EDS analysis of host grains, inclusions, lamellae, and intergrowths was conducted to determine the chemical composition of each phase present.

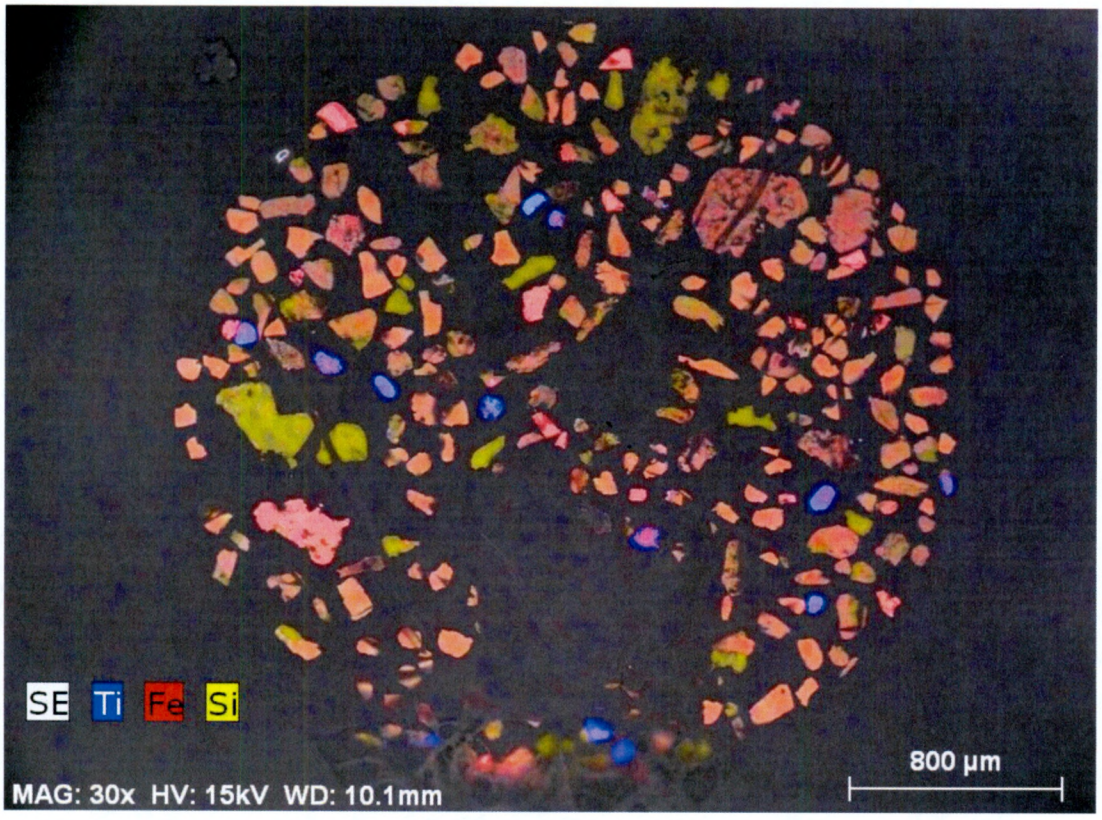

Figure 6. Color-coded X-ray map of grains from site MAM near the Foundation Ice Stream.

4. Atlas of Iron Oxide Textures and Compositions

The Fe oxide composition and texture identification process was based upon 1) comparison of wt% of each element derived from EDS analysis with stoichiometric wt% of each element within major minerals; and 2) identifying textures within the host grain.

4.1 Host Mineral Classification

Host minerals were assigned a mineral name based on the wt% of Fe, Ti, and O for Fe-oxide grains, and wt% Fe and S for iron sulfides. Magnetite was identified by its high wt% Fe (near to 72%), absence of Ti, and O wt% in the range of 27-28%. Titanomagnetite contains high Fe wt% (61-72%), low amounts of Ti (2-13%), and O wt% ranging from 27-28.5%. We use the term (titano)maghemite to describe a (titano)magnetite grain that has been oxidized but still retains its spinel mineral structure, as indicated by an intermediate O wt% of 28.5-30%. Hematite and titanohematite EDS spectra look nearly identical to magnetite and titanomagnetite, respectively. We identified (titano)hematite via its higher O content of 30-31 wt%.

Table 2. Stoichiometric Formulae and Element wt% for Fe-Ti Oxide Minerals

Mineral Name	Formula	wt% Fe	wt% Ti	wt% O
Magnetite	Fe_3O_4	72.36	-	27.64
TM10	$Fe_{2.9}Ti_{0.1}O_4$	70.19	2.07	27.73
TM20	$Fe_{2.8}Ti_{0.2}O_4$	68.01	4.16	27.83
TM30	$Fe_{2.7}Ti_{0.3}O_4$	65.81	6.27	27.93
TM40	$Fe_{2.6}Ti_{0.4}O_4$	63.59	8.38	28.03
TM50	$Fe_{2.5}Ti_{0.5}O_4$	61.36	10.52	28.12
TM60	$Fe_{2.4}Ti_{0.6}O_4$	61.57	12.67	28.22
Hematite	Fe_2O_3	69.94	-	30.06
TH10	$Fe_{1.9}Ti_{0.1}O_3$	66.78	3.01	30.21
TH30	$Fe_{1.7}Ti_{0.3}O_3$	60.36	9.13	30.51
Ilmenite	$FeTiO_3$	36.81	31.55	31.64
Rutile	TiO_2	-	59.93	40.07

TM = titanomagnetite ($Fe_{3-x}Ti_xO_4$), TH = titanohematite ($Fe_{2-y}Ti_yO_3$).

Ilmenite is characterized by similar wt% of Fe, Ti, and O (36.81%, 31.55%, and 31.64% respectively for stoichiometric ilmenite). The term ferrian ilmenite is given to ilmenite grains where the Fe content is greater than 37%. Rutile is named for its high percentage of Ti (>58%) and high O (near 40%), and little to no Fe. However, rutile observed in this study also contained small amounts (< 2 %) of Mg or Mn.

Fe sulfides were rare in these samples, but several forms were observed including framboids within sedimentary lithic grains. The Fe-sulfide grains were often part of multi-phase intergrowths and/or were smaller than the EDS interaction volume of 5 μm. Fe-sulfide stoichiometric formulae and wt% Fe and wt% S are included in Table 3, though in most cases we are unable to confidently identify the specific mineral phase. When present as framboids, we assume these were originally pyrite, though EDS spectra

containing oxygen suggest that the pyrite has been partially replaced by magnetite (Suk et al., 1990).

Table 3. Formulae and Element wt% for Stoichiometric Fe-sulfide Minerals

Mineral Name	Formula	wt% Fe	wt% S
Troilite	FeS	63.53	36.47
Pyrite	FeS_2	46.55	53.45
Pyrrhotite	Fe_7S_8	60.38	39.62
Hexagonal Pyrrhotite	Fe_9S_{10}	61.06	38.94
Greigite	Fe_3S_4	56.64	43.36

Table 4 presents formulae and wt% for other notable minerals observed in these samples. Fe-spinel describes minerals that resemble magnetite and titanomagnetite with respect to Fe and O wt%, but which contain spinel-group elements such as Al, Mg, and Cr in place of Ti. Other impurities present include Ca and V. Titanite is used to describe Ca-Ti silicates. While not expected to be magnetic, the presence of titanite in our magnetic fraction suggests it contains magnetic inclusions or intergrowths. Psilomelane and hausmannite are Mn-bearing minerals that are present in the till samples. We assigned the name psilomelane to Mn- and Ba-bearing oxides, and the name hausmannite to Mn-oxides, though small amounts of other cations are present in both of these minerals.

Table 4. Formulae and Element wt% for Other Minerals of Interest

Mineral Name	Formula	wt% Ti	wt% O	wt% Mg	wt% Mn	wt% Al	wt% Ba	wt% Si	wt% Ca
Hausmannite	Mn_3O_4	-	27.96	-	72.03	-	-	-	-
Psilomelane	$BaMn_9O_{16}(OH_4)$	-	26.78	-	51.73	-	14.36	-	-
Spinel	$(Fe,Al,Mg,Cr)_3O_4$	-	27-28	var	-	var	-	-	-
Titanite	$CaTiSiO_5$	24.42	40.82	-	-	-	-	14.33	20.41

var = variable

4.2 Fe Oxide Textures

Below is a gallery of Fe-oxide textures observed in the till samples from the Weddell Sea Sector (Fig. 7A-J). While this is not all-inclusive, these images represent the major textures we observed and are used here to illustrate the features that form the basis of textural classification names.

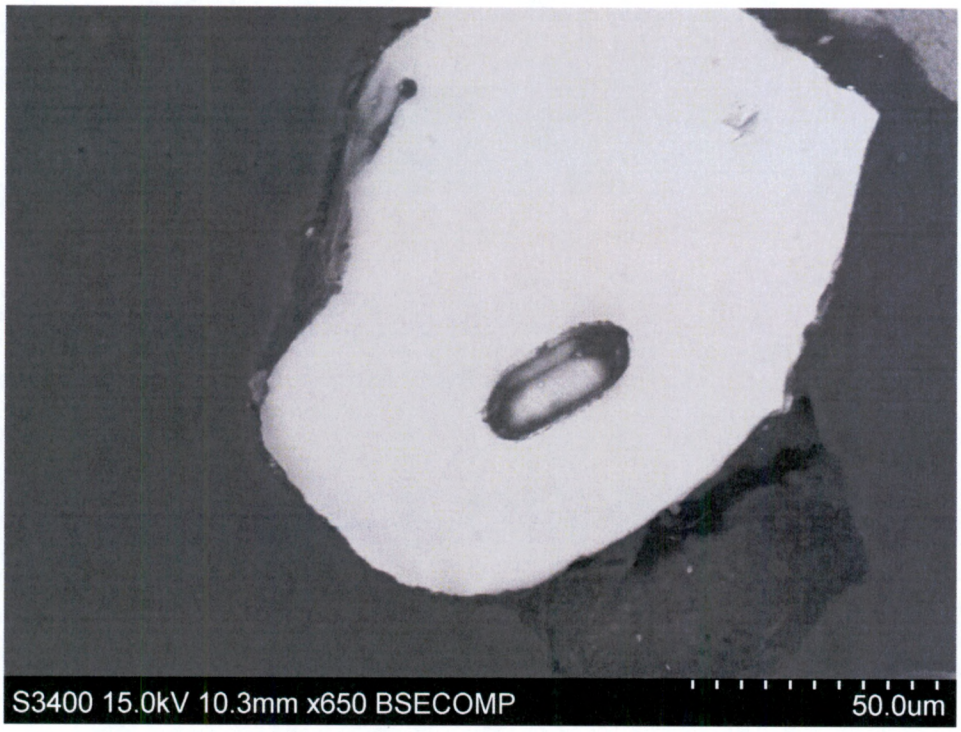

Figure 7A. Homogeneous Texture. There are no visible exsolution bodies or noteworthy features on, or within, the grains. This example is an ilmenite grain. The oval feature is likely a scar from plucking out another mineral grain (WAW2 near Recovery Ice Stream).

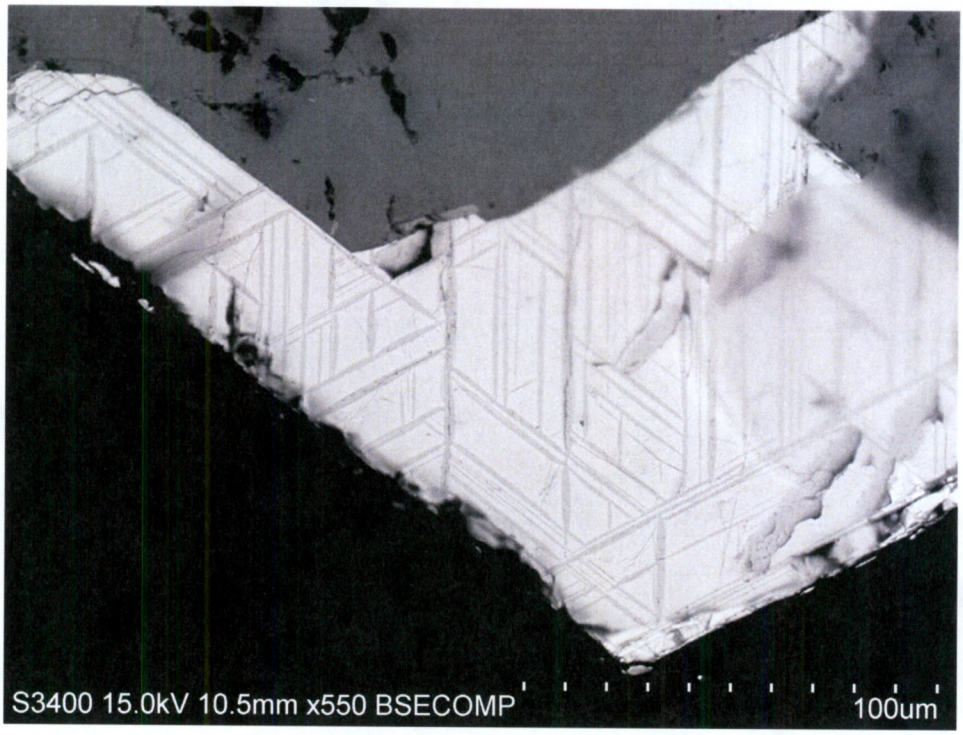

Figure 7B. Trellis Texture. The host contains continuous intergrowths or lamellae that span the whole grain. Grains may contain 1 to 4 swarms of lamellae. This example is a titanomagnetite host containing 4 swarms of ilmenite lamellae (MOU near Foundation Ice Stream).

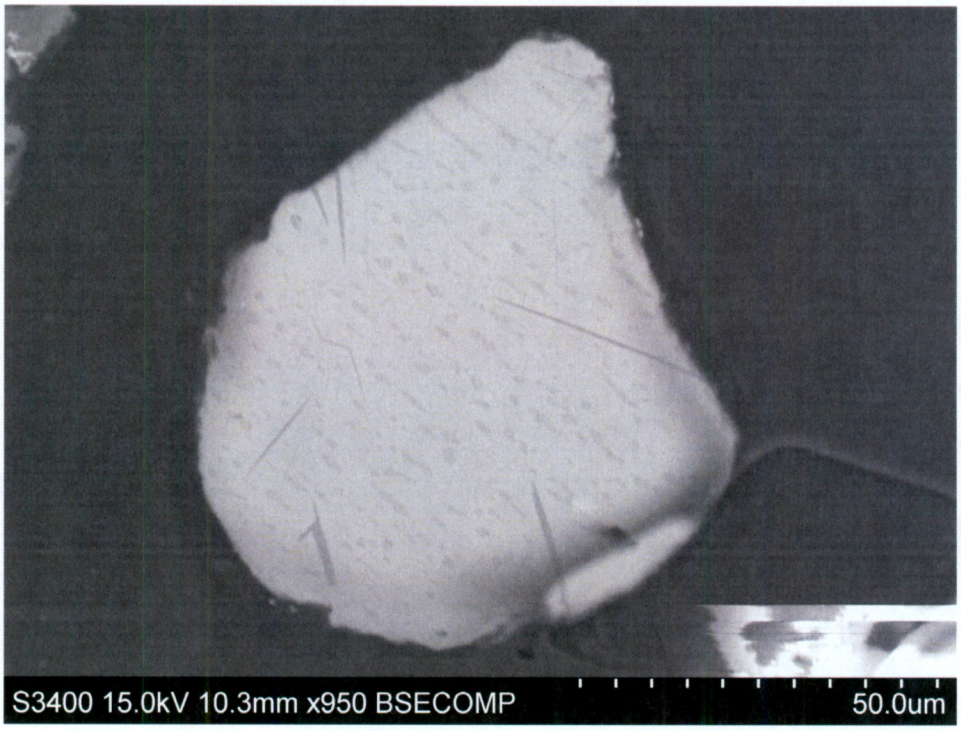

Figure 7C. Exsolution Texture. The host contains discontinuous intergrowths such as blebs, needles, and lenses. This example is a titanomagnetite host containing multiple ilmenite blebs and needles (YAR4C from Foundation Ice Stream).

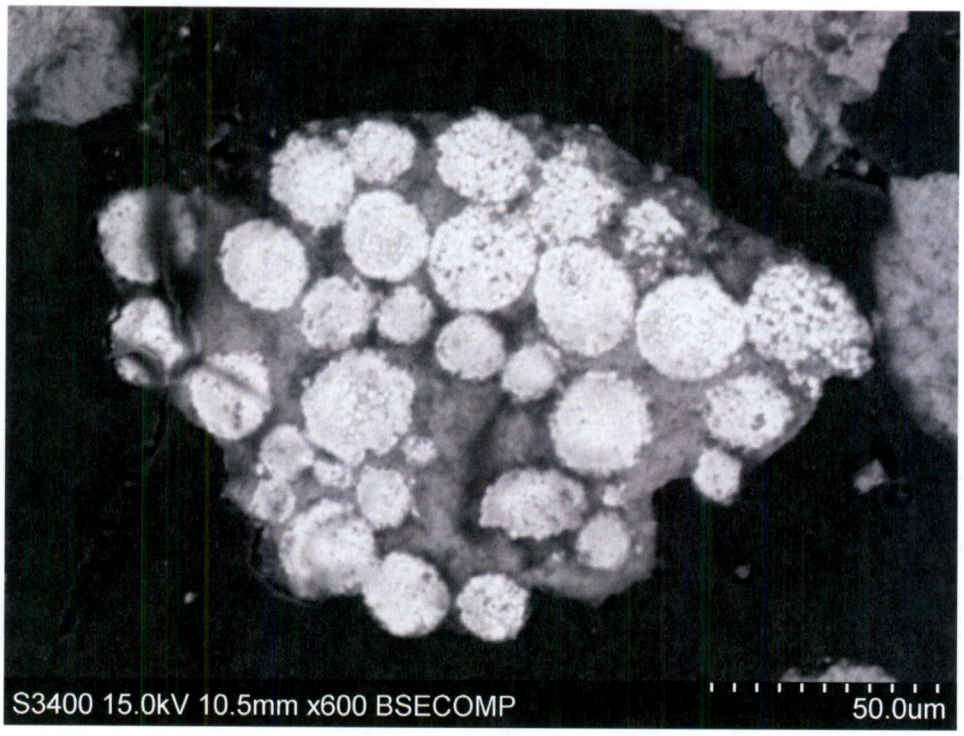

Figure 7D. Framboidal Texture. Framboids within sedimentary lithic clasts. We infer that these were originally pyrite framboids, but many of the observed grains show replacement by magnetite (WEB from Academy Glacier).

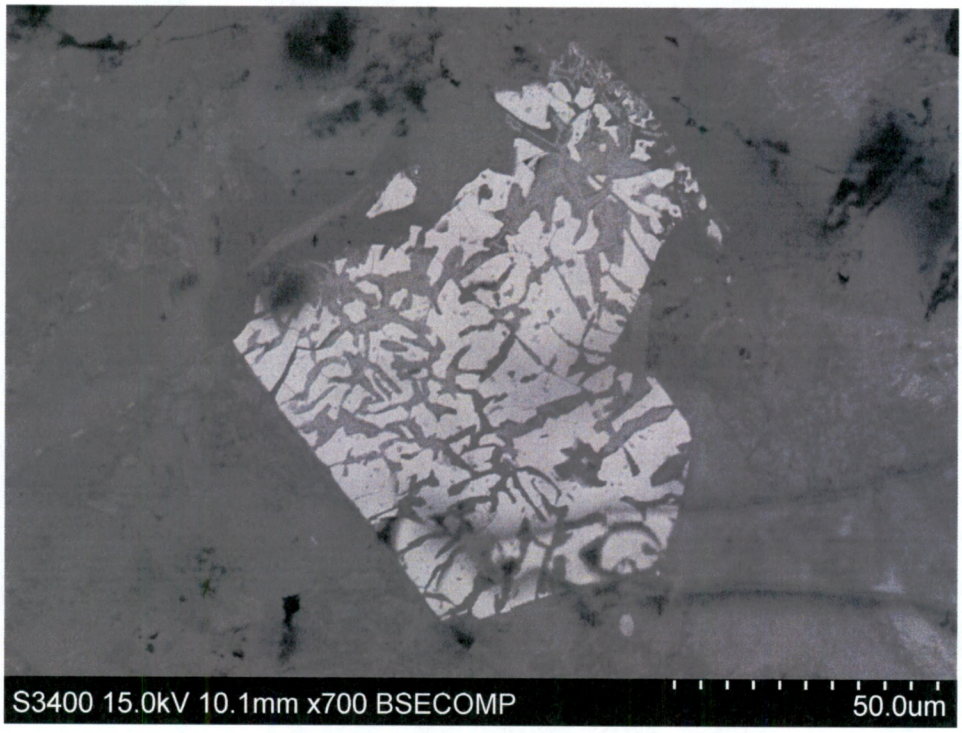

Figure 7E. Myrmekitic Texture. "Wormy" micron to submicron scale intergrowths of multiple minerals in a host grain. This example is a titanohematite host with Ca-rich silicate intergrowths (MAM2 from Foundation Ice Stream).

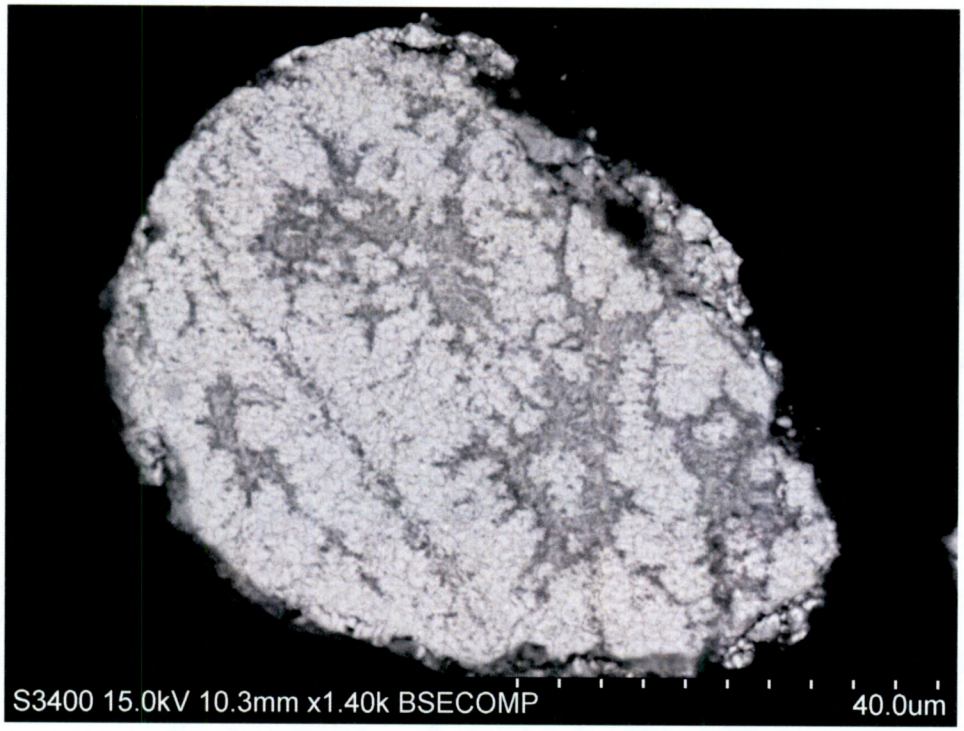

Figure 7F. Alteration Texture. The host grain chemistry and/or texture has been modified, presumably by oxidation, chemical weathering, or hydrothermal alteration of the bedrock that supplied the grain. Alteration is suggested in the BSE images by changing shades of grey along mineral twins, along grain boundaries and lamellae boundaries, or along cracks in the grain. These are interpreted as chemical changes propagating through the grain. This was the most abundant and the most variable Fe-oxide texture observed. This example is a Ti-rich ilmenite host with silicate alteration zones (YAR4A from Foundation Ice Stream).

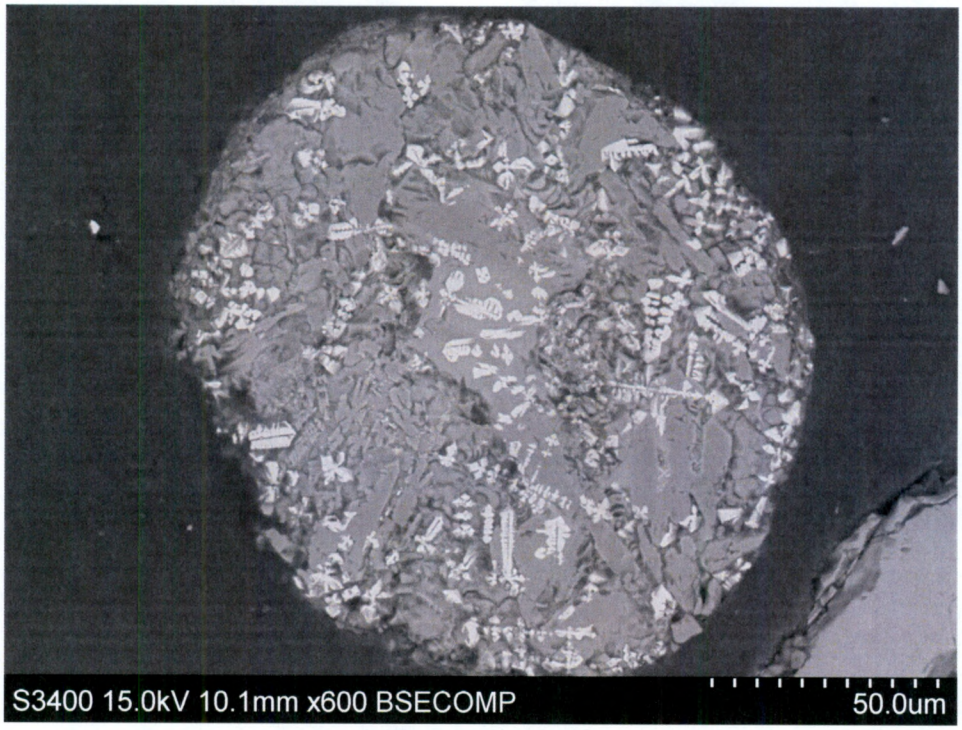

Figure 7G. Extrusive igneous texture. This term describes Fe-oxides within basalt lithic fragments. The Fe-oxide grains (bright white) are euhedral or have skeletal crystal forms. This example is a basalt lithic clast containing multiple skeletal magnetite crystals (YAR4A from Foundation Ice Stream).

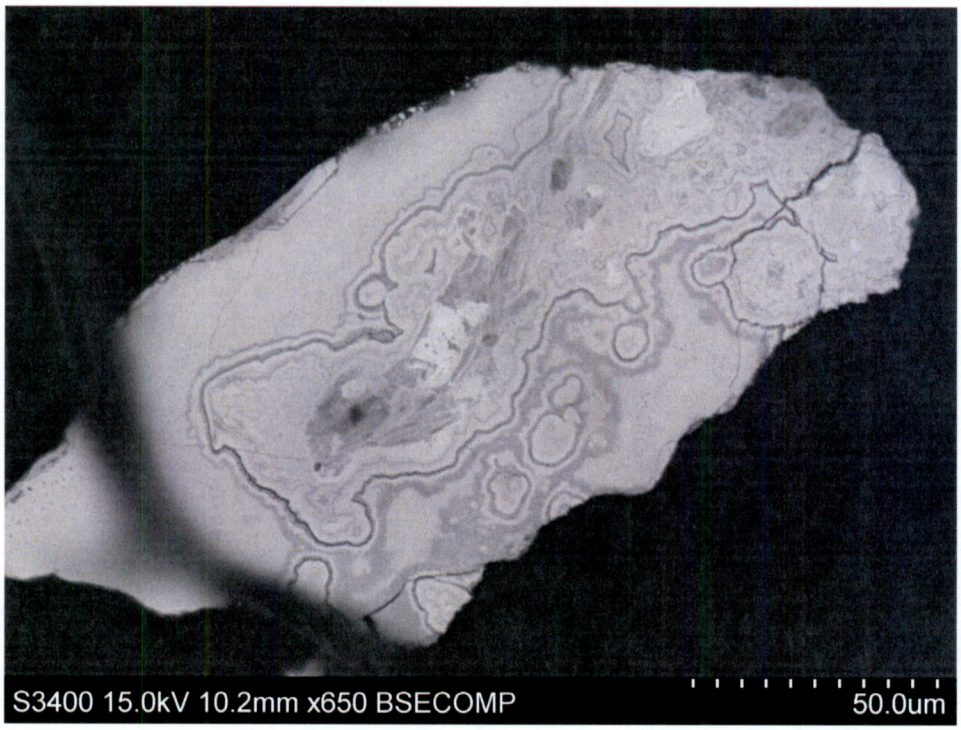

Figure 7H. Botryoidal Texture. Globular texture with circular ringlets of varying shades within a host grain. This example is a hematite host containing silicate and apatite banding (WAW2 from Recovery Ice Stream).

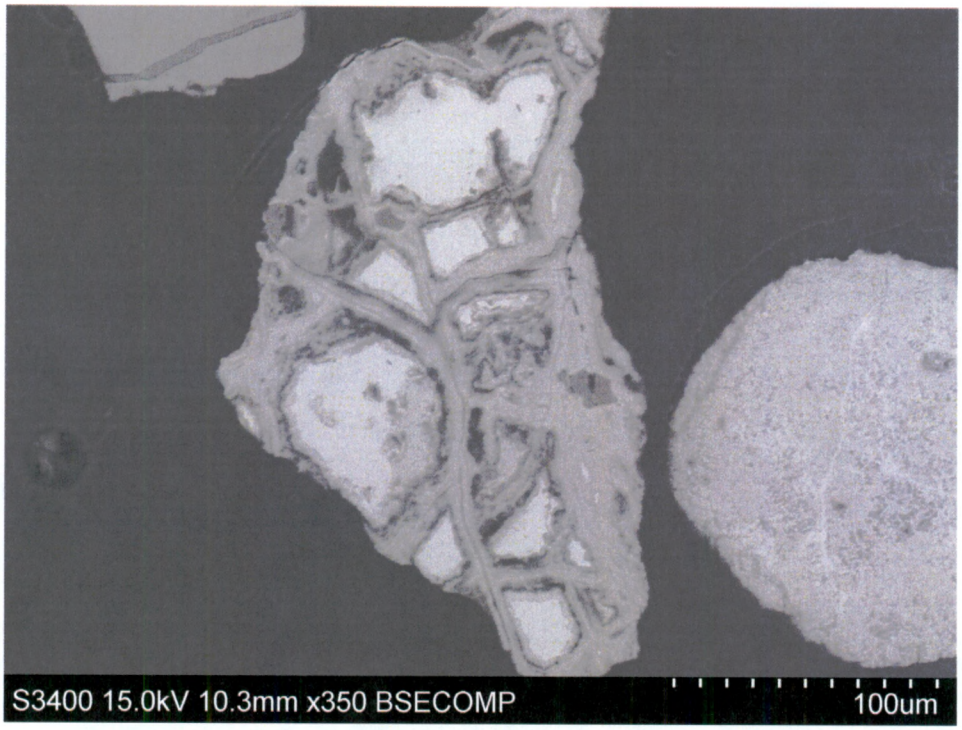

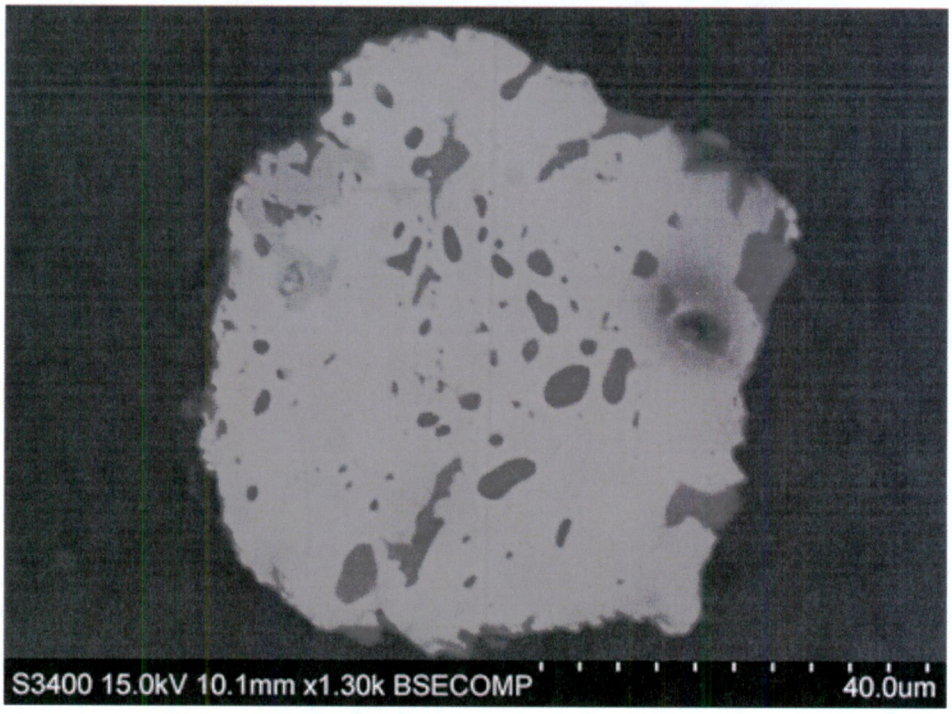

Figure 7I and 7J. Other Texture. "Other" describes those grains that are unlike any other textures previously listed or which have multiple textures. 7I is an example of an Fe-sulfide host with aluminosilicate and titanomagnetite inclusions and banding (YAR4C from Foundation Ice Stream). 7J is an example of an ilmenite host with aluminosilicate inclusions (MAM from Foundation Ice Stream).

5. Results

5.1. Study Area 1 – Foundation Ice Stream

5.1.1. Geochemistry

Major and trace element results for the < 63 μm sieve fraction are shown in Tables 5a-c. Spider diagrams were generated for major elements for each ice stream using wt% oxide data normalized such that the oxides sum to 100%. Major element oxides were normalized by average upper continental crust composition of Taylor and McLennan (1985). A larger number of samples were collected from along Foundation Ice Stream (Fig. 8) and there is variability within the sample set. Most of the mud fraction sediment samples are very similar to average continental crust composition, though with depletion of Ca and Na. The till in this ice stream has a greater range of elemental ratios when compared to the two other ice streams. The Al/Ti ratios range from 15 to 21, the Fe/Ti ratios range from 6.5 to 10.5, and the CIA values range from 55 to 68 with an average of 59.41 ± 4.17 (Table 5a). With exception of Ca and Na, all oxide ratios are very close to 1, indicating a composition very similar to average upper continental crust.

Table 5a. Major and Trace Element Results for the Foundation Ice Stream. Major element results are represented in weight percent oxides. Trace element results are represented in parts per million (ppm).

ICP-OES - Major Elements (wt %)														
Sample	YAR2 Till	YAR3 Till	YAR 4A	YAR 4B	YAR 4C	MAM Till	MAM2 Till	SUY Till	HEM Till	SIS Till	SIS2 Till	MAR Till	MOU Till	MOU2 Till
Ice Stream	Foundation	Foundation	Foundation	Foundation	Foundation	Foundation	Foundation	Foundation	Foundation	Foundation	Foundation	Foundation	Foundation	Foundation
SiO2	67.13	65.25	66.64	66.19	70.21	71.02	70.15	61.58	65.77	72.53	67.39	67.47	73.45	69.61
TiO2	0.72	0.70	0.75	0.79	0.78	0.72	0.75	0.80	0.70	0.69	0.76	0.69	0.74	0.72
Al2O3	16.34	16.73	16.57	16.14	15.24	14.58	14.16	18.70	16.06	13.46	16.40	16.05	12.25	15.07
Fe2O3	5.63	5.51	5.41	5.69	5.45	4.88	4.47	7.01	5.37	4.20	5.76	5.52	4.01	4.91
MnO	0.07	0.07	0.07	0.07	0.07	0.06	0.06	0.08	0.07	0.06	0.07	0.06	0.06	0.06
MgO	2.47	2.62	2.41	2.68	2.32	2.10	1.92	3.10	2.55	1.90	2.55	2.43	1.65	2.08
CaO	2.06	3.60	2.69	2.92	0.63	1.67	3.64	2.37	4.00	2.48	1.48	2.40	3.59	2.35
Na2O	0.95	0.74	0.73	1.05	1.17	0.89	0.60	1.30	0.78	0.59	0.96	0.98	0.58	0.69
K2O	4.45	4.61	4.53	4.29	3.94	3.90	4.05	4.88	4.54	3.89	4.45	4.24	3.44	4.32
P2O5	0.20	0.18	0.20	0.19	0.20	0.18	0.20	0.18	0.17	0.20	0.19	0.17	0.23	0.19
ICP-MS - Trace Elements (ppm)														
Sample	YAR2 Till	YAR3 Till	YAR 4A	YAR 4B	YAR 4C	MAM Till	MAM2 Till	SUY Till	HEM Till	SIS Till	SIS2 Till	MAR Till	MOU Till	MOU2 Till
Ice Stream	Foundation	Foundation	Foundation	Foundation	Foundation	Foundation	Foundation	Foundation	Foundation	Foundation	Foundation	Foundation	Foundation	Foundation
Sc	12.29	13.38	11.98	11.24	12.92	11.50	11.23	18.04	1.41	1.14	13.81	13.17	10.42	12.37
V	72.19	78.40	70.39	67.22	75.39	65.89	70.31	99.37	8.07	6.19	79.87	74.40	59.60	75.08
Co	12.16	12.64	11.57	10.96	12.63	10.54	10.09	18.15	1.28	0.96	12.60	14.02	9.17	11.55
Ni	23.24	27.00	26.78	21.26	21.52	19.38	18.90	32.20	2.48	1.76	24.20	21.73	14.45	21.08
Ga	19.67	20.72	19.51	19.16	20.25	18.85	18.48	26.21	2.17	1.78	20.80	20.86	15.85	19.35
Rb	179.36	193.32	177.41	167.24	179.01	166.35	167.45	241.91	19.49	16.33	188.73	190.43	134.83	180.99
Sr	63.51	162.72	78.73	65.80	58.85	63.54	82.81	84.00	21.00	11.29	79.78	84.91	86.02	73.37
Y	39.00	40.57	39.37	36.23	41.10	39.17	45.42	48.03	4.16	4.23	40.50	40.02	44.41	42.66
Zr	248.63	274.84	298.42	198.23	300.10	269.69	302.42	209.46	32.04	44.93	332.97	247.72	520.86	334.90
Nb	12.03	12.65	12.64	13.27	14.81	13.54	13.88	18.61	1.35	1.26	13.65	13.30	12.62	13.05
Cs	9.91	10.38	10.12	10.01	11.07	8.77	8.29	23.34	1.09	0.85	11.74	11.47	6.38	10.10
Ba	518.38	595.82	559.22	523.42	592.89	526.25	554.91	635.45	61.25	54.15	548.63	608.36	480.13	582.40
La	42.47	47.23	48.23	44.64	47.32	46.01	54.52	48.62	5.01	4.95	45.95	46.57	49.98	50.67
Ce	96.94	106.37	112.88	102.36	114.94	105.44	124.22	114.23	11.30	11.32	103.84	108.79	115.93	116.40
Pr	10.81	11.64	12.06	11.21	12.07	11.48	13.43	12.44	1.23	1.22	11.38	11.62	12.68	12.47
Nd	40.84	44.54	45.16	42.06	45.77	43.70	50.96	48.47	4.58	4.57	43.02	44.01	48.22	46.86
Sm	8.08	8.75	8.98	8.23	9.12	8.60	10.16	10.08	0.89	0.90	8.48	8.85	9.45	9.25
Eu	1.37	1.50	1.49	1.39	1.52	1.40	1.66	1.70	0.15	0.14	1.46	1.43	1.49	1.50
Tb	1.14	1.26	1.25	1.16	1.28	1.24	1.43	1.48	0.13	0.13	1.23	1.24	1.34	1.30
Dy	6.61	6.83	6.83	6.31	7.18	6.78	7.75	8.16	0.72	0.73	6.80	6.89	7.50	7.30
Ho	1.34	1.43	1.41	1.33	1.48	1.41	1.65	1.73	0.15	0.15	1.40	1.43	1.56	1.50
Er	3.82	4.04	3.92	3.59	4.06	3.89	4.40	4.73	0.42	0.43	4.00	3.91	4.38	4.26
Tm	0.57	0.61	0.62	0.55	0.63	0.62	0.68	0.73	0.07	0.07	0.62	0.63	0.68	0.65
Yb	3.62	3.84	3.73	3.47	3.92	3.75	4.18	4.77	0.41	0.41	3.91	3.83	4.27	4.07
Lu	0.54	0.59	0.58	0.53	0.61	0.58	0.66	0.70	0.06	0.06	0.60	0.59	0.65	0.61
Hf	6.88	7.64	8.19	5.48	8.26	7.63	8.55	6.16	0.94	1.33	9.13	7.00	15.42	9.62
Ta	0.97	1.05	1.08	1.08	1.21	1.13	1.22	1.38	0.12	0.11	1.13	1.10	1.02	1.11
Pb	27.02	6.68	18.44	24.23	25.91	23.43	24.45	29.07	2.63	2.78	27.24	32.09	32.25	33.28
Th	16.62	18.60	19.17	16.84	18.07	17.47	20.12	21.28	2.04	1.87	17.85	17.94	17.23	19.59
U	3.21	3.77	3.99	3.79	3.71	3.08	3.90	6.11	0.41	0.41	3.63	3.36	3.70	3.67

Table 5b. Major and Trace Element Results for the Academy Glacier. Major element results are represented in weight percent oxides. Trace element results are represented in parts per million (ppm).

ICP-OES - Major Elements (wt %)				
Sample		WEB Till	LIC Till	LIC2 Till
Ice Stream		Academy	Academy	Academy
	SiO2	64.49	64.70	63.79
	TiO2	0.84	0.66	0.71
	Al2O3	18.09	18.03	18.39
	Fe2O3	6.95	5.72	5.77
	MnO	0.09	0.08	0.08
	MgO	3.05	2.02	2.03
	CaO	0.55	2.63	3.13
	Na2O	1.16	0.69	0.63
	K2O	4.59	5.26	5.28
	P2O5	0.19	0.19	0.19
ICP-MS - Trace Elements (ppm)				
Sample		WEB Till	LIC Till	LIC2 Till
Ice Stream		Academy	Academy	Academy
	Sc	16.35	13.66	12.94
	V	95.33	80.25	85.35
	Co	18.15	11.90	11.14
	Ni	31.28	22.11	35.40
	Ga	23.56	24.10	21.61
	Rb	214.14	225.10	197.25
	Sr	65.86	69.96	81.14
	Y	42.87	40.90	37.37
	Zr	202.44	245.16	226.84
	Nb	16.14	12.16	13.05
	Cs	15.75	7.82	8.85
	Ba	666.71	649.58	591.68
	La	46.60	49.47	45.25
	Ce	113.38	117.53	102.89
	Pr	12.07	12.55	10.97
	Nd	46.61	47.15	41.02
	Sm	9.49	9.33	8.24
	Eu	1.62	1.57	1.42
	Tb	1.36	1.29	1.17
	Dy	7.56	7.11	6.52
	Ho	1.58	1.43	1.35
	Er	4.27	3.91	3.64
	Tm	0.67	0.62	0.56
	Yb	4.11	3.78	3.52
	Lu	0.61	0.58	0.52
	Hf	5.62	7.03	6.24
	Ta	1.31	0.98	0.95
	Pb	31.23	32.14	20.59
	Th	18.79	21.50	18.73
	U	3.55	3.69	2.99

Table 5c. Major and Trace Element Results for the Recovery Ice Stream. Major element results are represented in weight percent oxides. Trace element results are represented in parts per million (ppm).

ICP-OES - Major Elements (wt %)					
Sample		STB Till	STB2 Till	WAW Till	WAW2 Til
Ice Stream					
	SiO2	69.79	70.20	60.62	60.10
	TiO2	0.67	0.63	1.33	1.19
	Al2O3	16.34	16.27	19.38	20.17
	Fe2O3	3.86	3.79	8.21	8.44
	MnO	0.02	0.02	0.09	0.09
	MgO	2.33	2.32	2.41	2.45
	CaO	0.28	0.25	1.51	1.50
	Na2O	0.97	0.96	2.63	2.30
	K2O	5.64	5.48	3.47	3.46
	P2O5	0.09	0.08	0.34	0.31
ICP-MS - Trace Elements (ppm)					
Sample		STB Till	STB2 Till	WAW Till	WAW2 Til
Ice Stream					
	Sc	14.34	13.30	21.31	20.12
	V	55.86	59.21	162.47	149.02
	Co	6.45	6.37	18.82	17.64
	Ni	9.47	8.03	44.13	42.76
	Ga	20.53	20.74	28.58	27.43
	Rb	209.30	202.94	152.50	142.25
	Sr	42.79	44.66	183.03	170.70
	Y	45.71	45.46	54.43	47.57
	Zr	473.85	332.95	453.24	314.44
	Nb	14.74	13.95	18.58	16.06
	Cs	6.50	6.58	5.65	5.42
	Ba	687.66	681.11	838.10	779.89
	La	51.61	55.27	77.17	62.55
	Ce	121.30	127.18	151.89	140.84
	Pr	13.16	13.96	19.30	15.60
	Nd	49.89	52.69	73.48	59.12
	Sm	9.77	10.14	14.07	11.57
	Eu	1.79	1.82	2.28	1.97
	Tb	1.33	1.37	1.84	1.54
	Dy	7.42	7.62	9.77	8.27
	Ho	1.62	1.63	2.00	1.70
	Er	4.76	4.60	5.38	4.59
	Tm	0.79	0.75	0.83	0.70
	Yb	5.16	4.82	4.89	4.31
	Lu	0.81	0.76	0.76	0.65
	Hf	14.35	9.26	13.06	8.43
	Ta	1.22	1.16	1.34	1.16
	Pb	8.34	17.24	23.39	18.28
	Th	19.50	20.12	27.46	22.40
	U	5.14	4.79	6.43	5.56

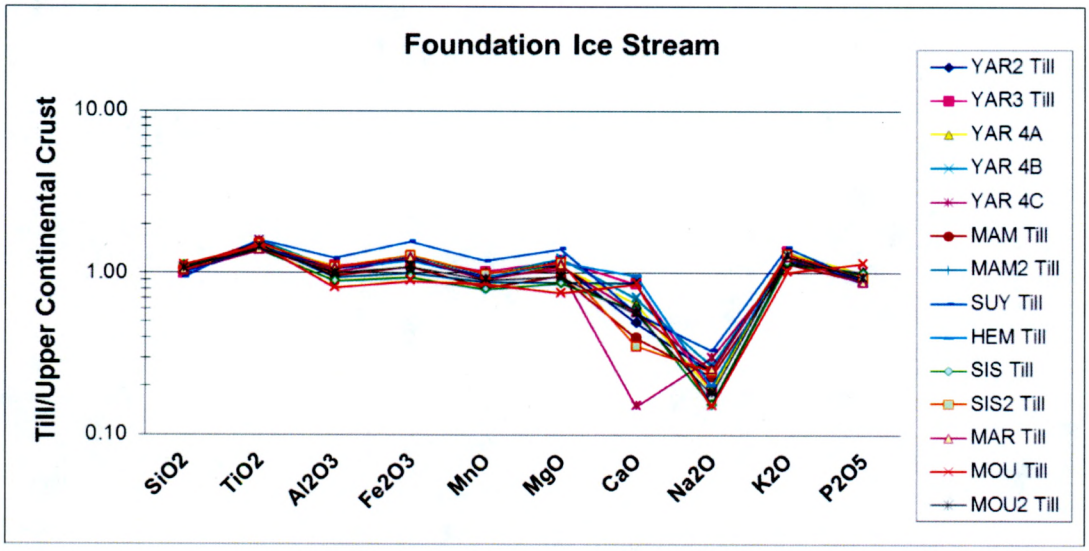

Figure 8. "Spider Diagram" of major element oxides in the mud fraction normalized by average upper continental crust composition of Taylor and McLennan, 1985. Foundation Ice Stream has overall depletion in Ca and Na.

5.1.2. Fe-Oxides

The dominant texture in Foundation Ice Stream samples is the alteration texture category (49%), followed by exsolved and trellis textures (23%), homogeneous texture (16%), and then the "other" category (8%). The next four textures were present in the Foundation Ice Stream, but did not exceed 1% of the total assemblage: Extrusive igneous texture, myrmekitic, botryoidal and framboid textures (Fig. 9).

The dominant host minerals are titanomagnetite (34%) and ilmenite (32%) followed by magnetite (18%). Hematite (4%), calcium titanite, and titanohematite (3% each) are present along with rutile (2%) and finally <1% each of maghemite and spinel (Fig.10).

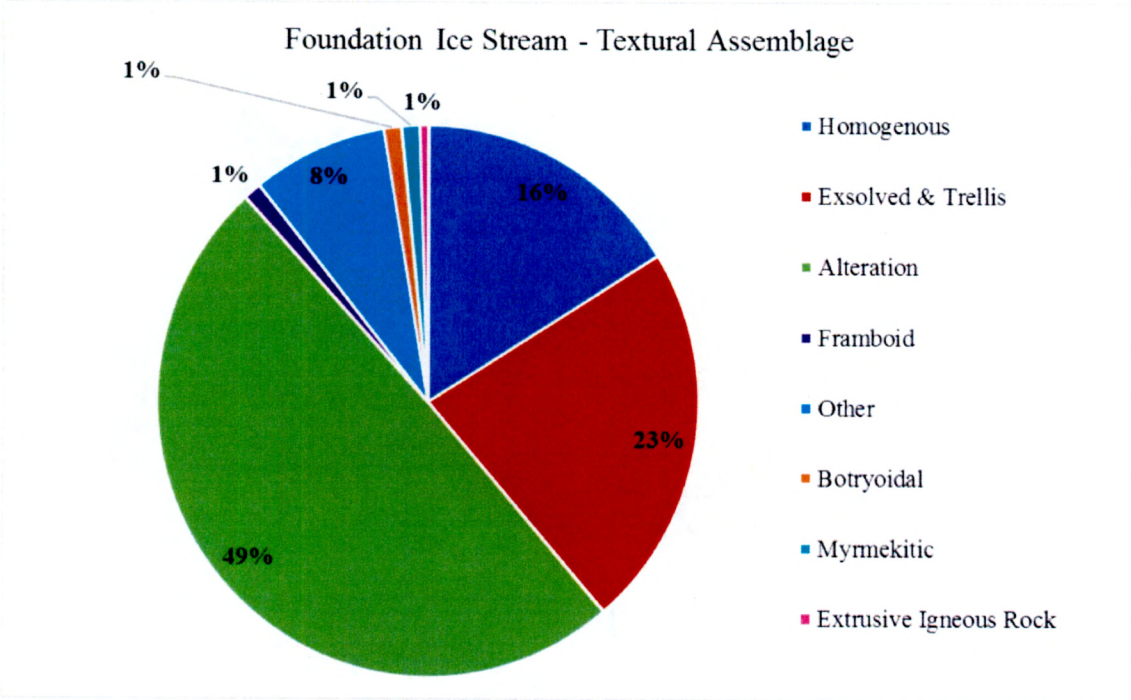

Figure 9. Foundation Ice Stream Fe-oxide textural assemblage. The assemblage is predominately composed of alteration, exsolved & trellis, and homogenous textures.

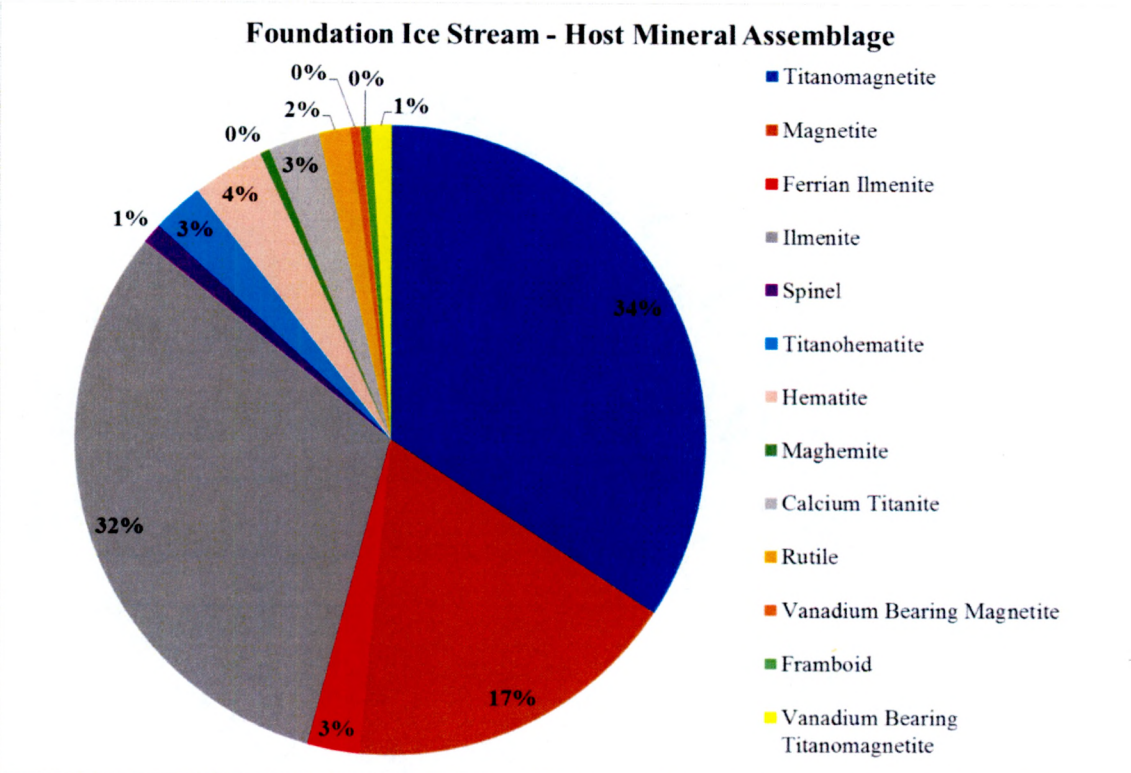

Figure 10. Foundation Ice Stream Fe-oxide host mineral assemblage. The majority of the assemblage is composed of titanomagnetite (34%), ilmenite (32%), and magnetite (17%).

5.2. Study Area 2 – Academy Glacier

5.2.1. Geochemistry

Academy Glacier till is very similar to the average crust composition, with slight depletion of Ca and strong depletion of Na (Fig. 11). The exception is WEB, from the Weber Ridge on the southern margin of Academy Glacier, which lies within the Patuxent Formation. WEB is strongly depleted in Ca and slightly more enriched in Ti, Fe, Mg, and K when compared to the two other sample sites. LIC and LIC2 are located on the north side of Academy Glacier within the Neptune Group, host to younger Ordovician sandstones. The till from northern Academy Glacier (LIC and LIC2) has the highest Al/Ti values (23-24) of the three ice streams studied, as well as the highest Fe/Ti values (9-10). The chemical index of alteration values range from 60.0 to 70.0, with an average of 63.37 ± 5.47 (Table 5b, 6).

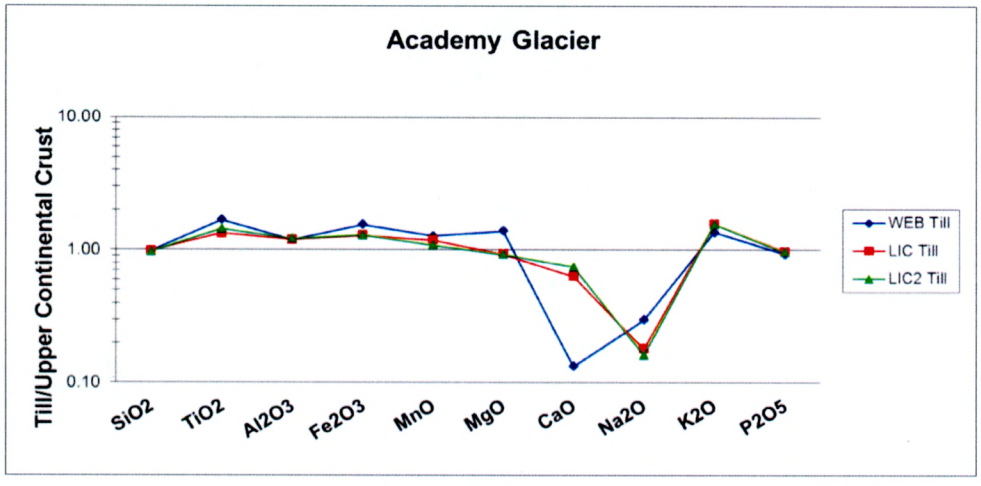

Figure 11. "Spider Diagram" of major element oxide concentrations in Academy Glacier till (mud fraction) normalized by average upper continental crust composition of Taylor and McLennan, 1985. All three sites are depleted in Ca and Na and have slight enrichment in Ti, Fe, and K. The WEB site shows greater Mg enrichment. Although there are no outcrops exposed, these patterns suggest the presence of mafic units under the ice.

5.2.2. Fe-Oxides

The dominant Fe-oxide texture observed in Academy Glacier samples is the alteration texture (63%), followed by the exsolved and trellis textures (26%), homogenous texture (7%) and finally the framboid structures (4%) (Fig. 12). The Academy Glacier host grain mineralogy consists of titanomagnetite (44%) followed by magnetite (30%). There is also maghemite present (7%) and small amounts of ferrian ilmenite (4%), Fe-Mg-Mn spinel (3%), titanomaghemite (3%), pyrite/magnetite framboids (3%), hematite (3%), and Al-bearing magnetite (3%) (Fig. 13).

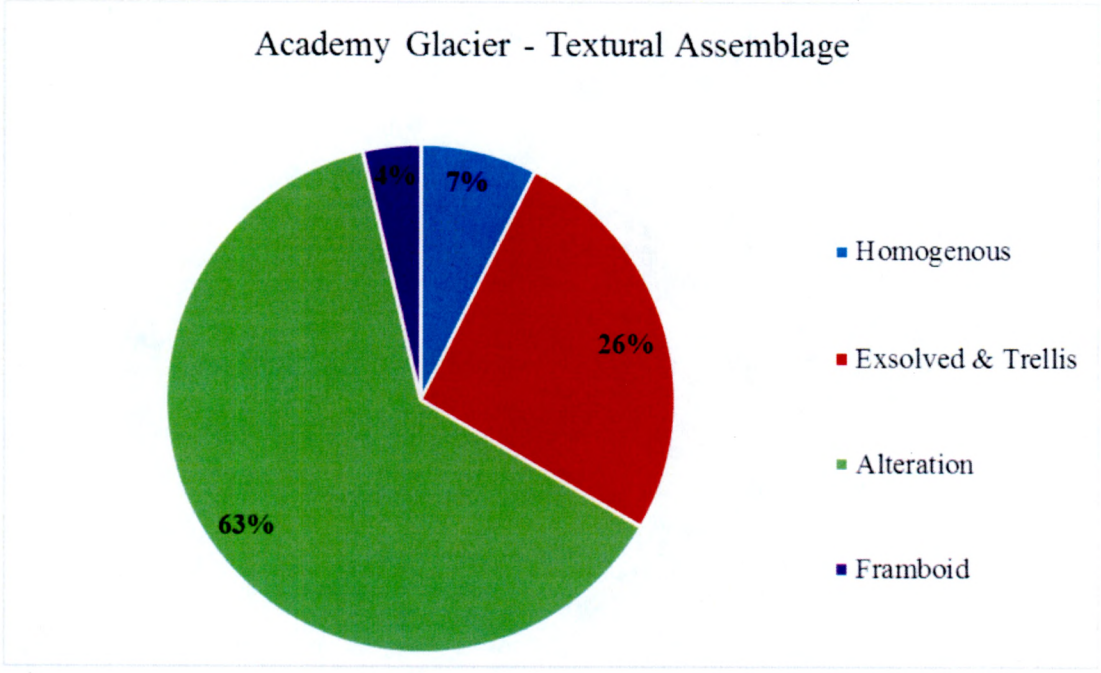

Figure 12. Academy Glacier Fe-oxide textural assemblage. The assemblage is predominately composed of alteration texture.

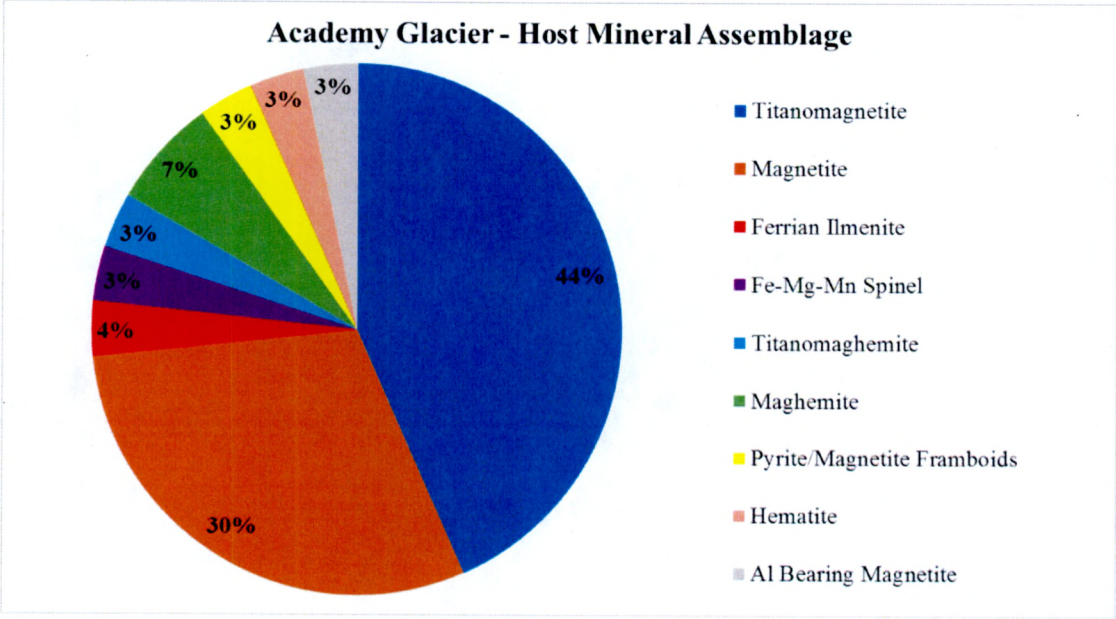

Figure 13. Academy Glacier Fe-oxide host mineral assemblage. The majority of the assemblage is composed of titanomagnetite (44%), magnetite (30%), and maghemite (7%).

3.3. Study Area 3 – Recovery Ice Stream

5.3.1. Geochemistry

Recovery Ice Stream is represented by 4 samples, two from the northern margin (STB and STB2, Fig 14) and two from the southern margin (WAW and WAW2, Fig. 15). Till mud fraction from the northern margin of the ice stream is slightly depleted in Mn, Ca and Na, but has high Al/Ti ratios (21-22) and high Fe/Ti ratios (6-9). Till from the southern margin is more enriched in mafic elements relative to the northern margin samples, has lower Al/Ti ratios (13-15), and elevated Mn/Al (0.0060-0.0065) and Fe/Al ratios (7.5-8.5). CIA values range from 63 to 68, with an average of ~66.04 ± 1.31 (Table 5c).

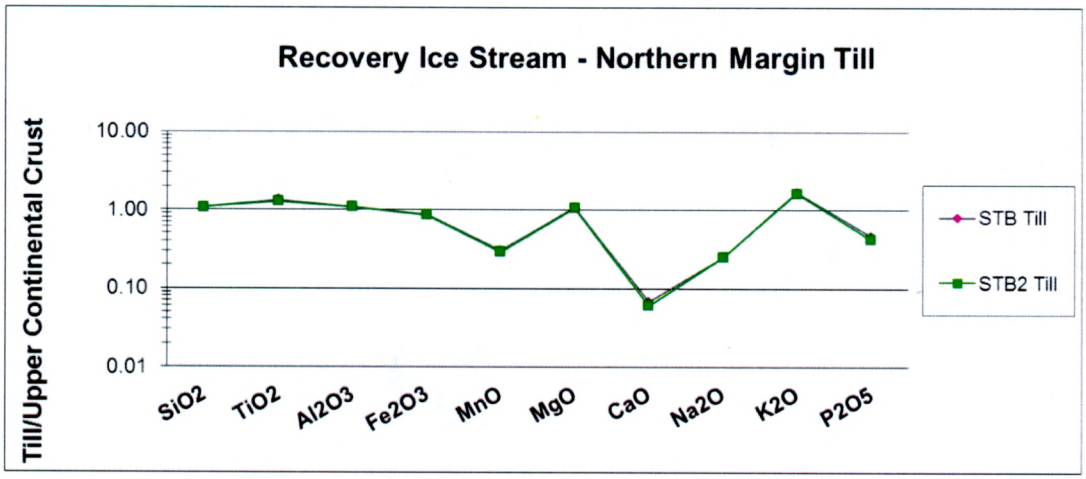

Figure 14. "Spider Diagram" of northern margin till mud fraction (STB and STB2) major elements normalized by average upper continental crust composition of Taylor and McLennan, 1985. The northern margin samples STB and STB2 are depleted in Mn, Ca and Na.

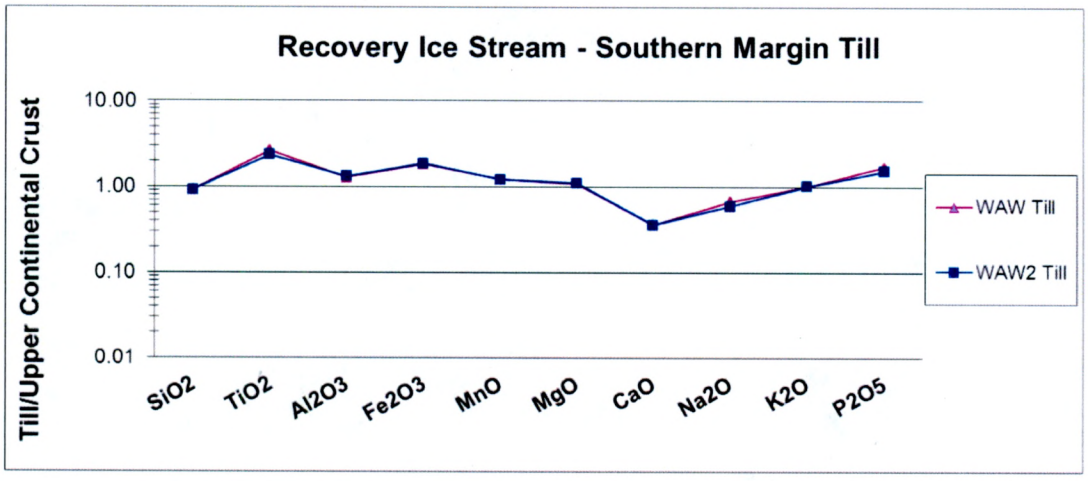

Figure 15. "Spider Diagram" of southern margin till mud fraction (WAW and WAW2) major elements normalized by average upper continental crust composition of Taylor and McLennan, 1985. Southern till is slightly more enriched in mafic elements than the northern margin sites, and are slightly less depleted in Ca and Na.

5.3.2 Fe-Oxides

Recovery Ice Stream is dominated by alteration texture (34%), followed by the exsolved and trellis texture (24%) and homogenous grains (24%). Other textures present include other (9%), framboid textures (7%), and botryoidal (2%) (Fig.16). The northern

margin till (STB and STB2) displays more exsolved and trellis textures than the southern margin till (WAW and WAW2). The southern margin till, on the other hand, displays significantly more homogeneous, framboidal, and botryoidal textures when compared to the northern till samples (Fig. 17).

Host minerals for this site are varied and numerous, however, the most dominant mineral is titanomagnetite (35%), followed by hematite (15%), Ca- and Mn-bearing magnetite (12%), rutile (7%), and ilmenite (7%). Also present are Mg- and Al-bearing titanomagnetite (3%), ferrian rutile (3%), Mn- bearing ilmenite (3%), magnetite (3%), and Mg-bearing magnetite (3%). Finally, host minerals that are present but comprise < 2% of the total assemblage are titanohematite, hausmannite, ferrian ilmenite, psilomelane, and Fe- and Al- bearing rutile (Fig.18). The northern and southern tills show a few distinct differences between them; the southern till contains more Ca- and Mn- bearing magnetite, hematite, and Mg- bearing magnetite. WAW and WAW2 are the only sites from Recovery Ice Stream, and in the entire sample set, that contain psilomelane and hausmannite. The northern till is distinct from the southern till as it contains significantly more titanomagnetite, rutile, Mn- bearing ilmenite, and Mg- bearing magnetite (Fig. 19).

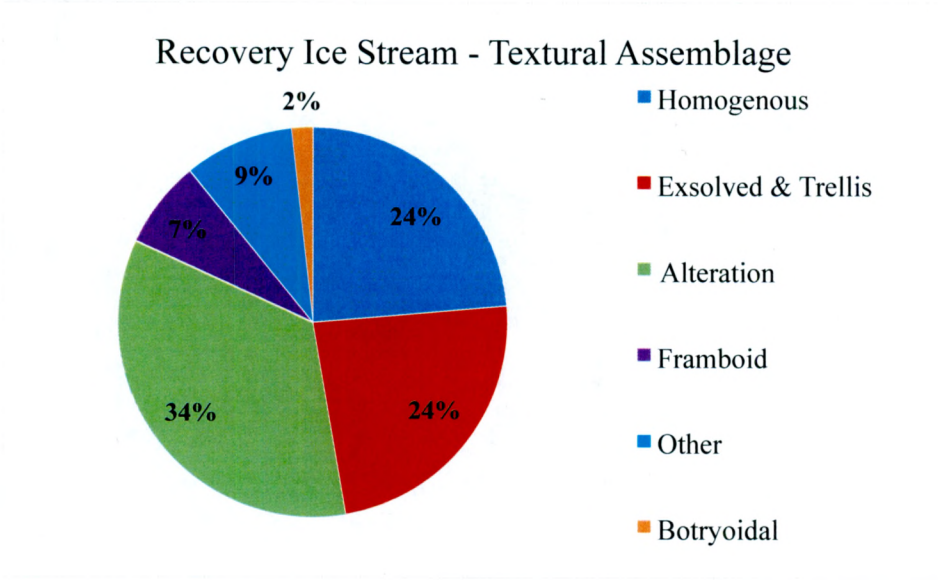

Figure 16. Recovery Ice Stream Fe-oxide textural assemblage. The assemblage is predominately composed of alteration, exsolved & trellis, and homogenous textures.

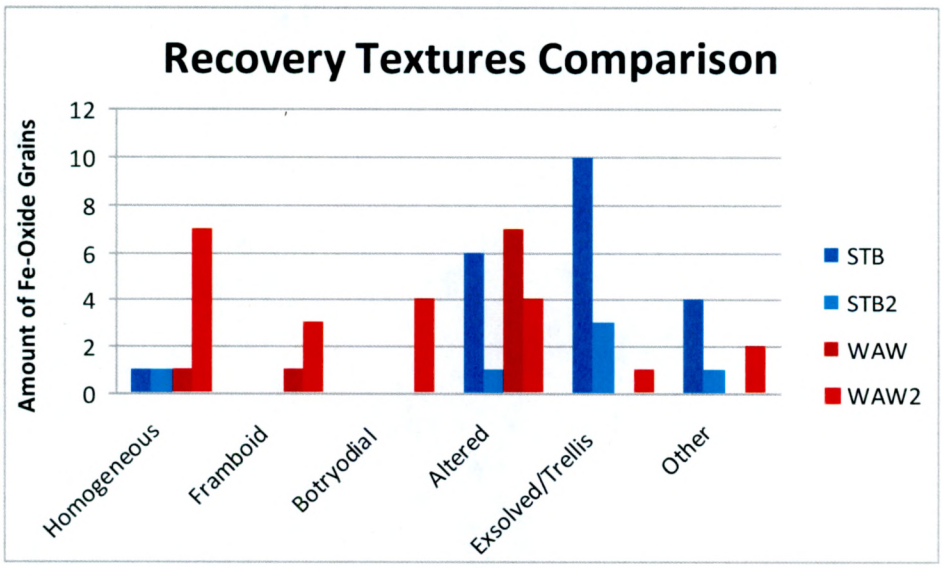

Figure 17. Recovery Ice Stream Fe-oxide textual assemblage comparison between northern till (STB and STB2; blue) and southern till (WAW and WAW2; red).

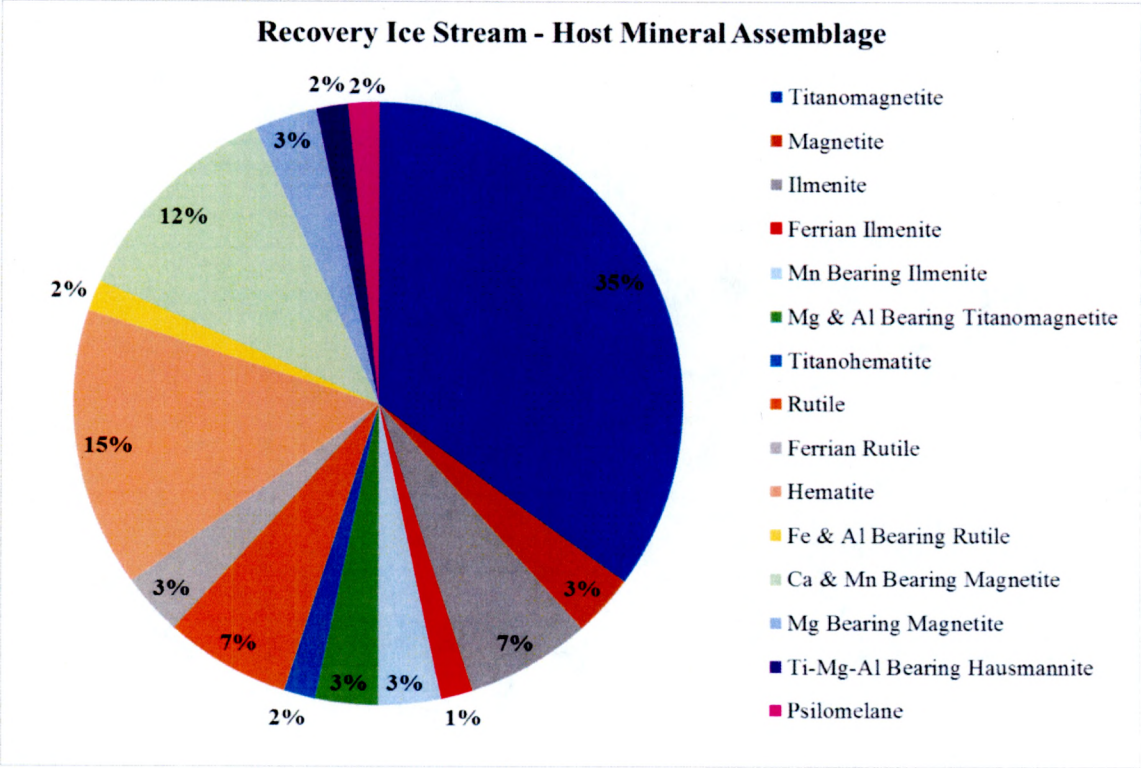

Figure 18. Recovery Ice Stream Fe-oxide host mineral assemblage. The ice stream is composed of titanomagnetite (35%), hematite (15%), and Ca & Mg bearing magnetite (12%).

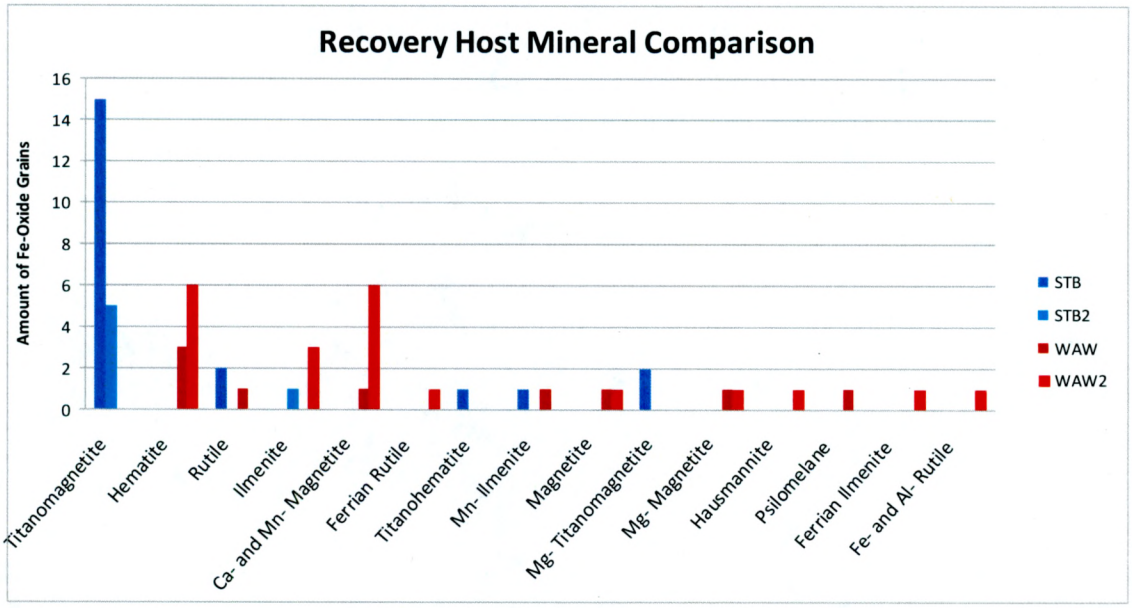

Figure 19. Recovery Ice Stream Fe-oxide host mineral assemblage comparison between northern till (STB and STB2; blue) and southern till (WAW and WAW2; red).

6. Discussion

Till from all three ice streams have Al/Ti values consistent with upper continental crust sources rocks (Table 6). Average Al/Ti ratios from Academy Glacier (21.9± 2.57) are higher than the average Foundation (19.2 ± 1.86) and Recovery (18.0± 4.85) Ice Stream values. Average Fe/Ti ratios from Academy Glacier (9.7 ± 0.33) are higher than Foundation Ice Stream (8.3 ± 1.06) and Recovery Ice Stream (7.3 ± 0.69) values. The Chemical Index of Alteration (CIA) values were calculated according to Nesbitt and Young (1982). In this study we observe that CIA values increase from west to east, with 59.41 ± 4.17 observed in Foundation Ice Stream, 63.3 ± 5.47 observed in Academy Glacier, and 66.06 ± 1.31 observed in Recovery Ice Stream. Neither the major element ratios or CIA values are sufficiently distinct to identify individual ice streams once sediments are deposited and mixed in the ocean. However, CIA values are consistent with physical weathering of the bedrock rather than local reworking of sediment. This suggests that our geochemical data is a reliable bedrock signature. However, trace element data from our ICP-MS dataset is likely better suited to this purpose than major elements. Principal Component Analysis of the trace element data will comprise post-thesis work.

Table 6. Summary of Provenance Tracer Data

Ice Stream	Al/Ti Range Avg ± std	Fe/Ti Range Avg ± std	CIA Range Avg ± std	Major Fe-oxide textures	Major host minerals
Foundation	15 to 21	6.5 to 10.5	55 to 68	AL (49%)	Titanomagnetite, Magnetite, and Ilmenite
	19.20 ± 1.86	8.36 ± 1.06	59.41 ± 4.17	ET (23%)	
				HO (16%)	
Academy	23 to 24	9 to 10	60.0 to 70.0	AL (63%)	Titanomagnetite and Magnetite
	21.9 ± 2.57	9.73 ± 0.33	63.37 ± 5.47	ET (26%)	
Recovery	13 to 23	6.3 to 8.3	64 to 67	AL (34%)	Titanomagnetite, Psilomelane, and Hausmannite
	18 ± 4.85	7.31 ± 0.69	66.04 ± 1.31	ET (24%)	
				HO (24%)	

AL = alteration texture; ET = exsolved + trellis; HO = homogeneous

All three ice streams show depletion in Ca and Na relative to the average continental crust. Calcium and sodium are easily leachable elements that are prime indicators of weathering as feldspar minerals are weathered to clay minerals. The depletion seen within these ice streams may be indicating weathering of plagioclase feldspar in the bedrock and/or sediments below the ice.

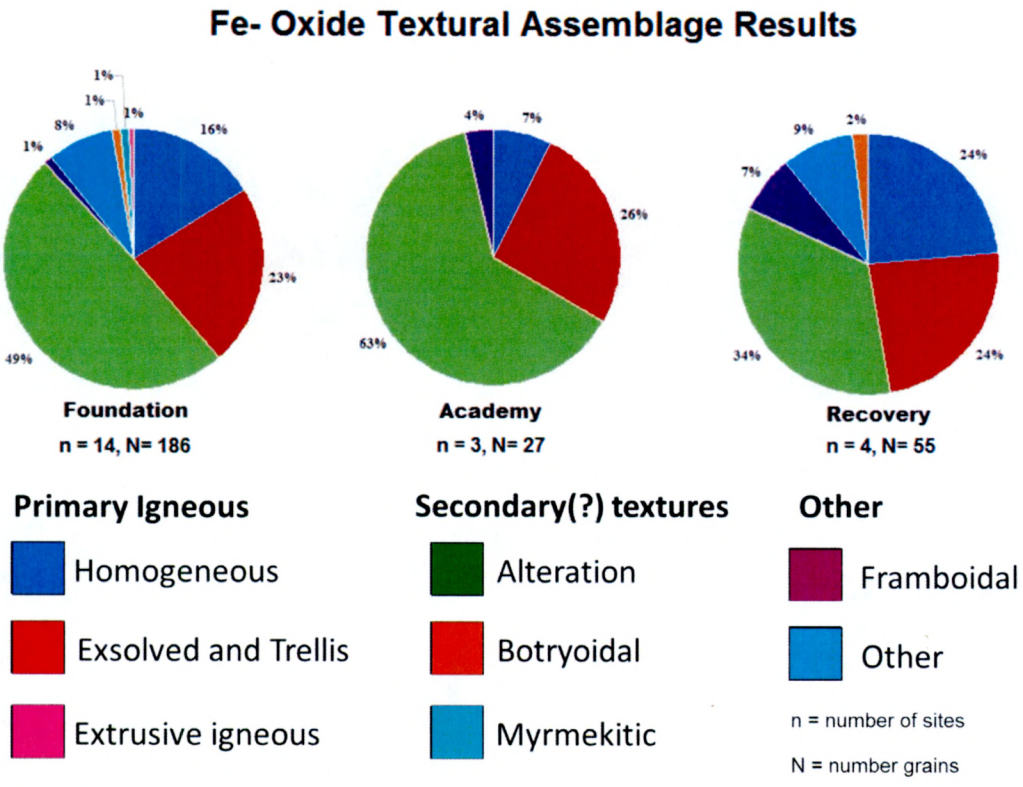

Figure 20. Comparison of Fe-oxide textural assemblages. The Academy Glacier, an Fe-oxide poor ice stream, yields the most alteration texture. The Recovery Ice Stream yields the least amount of alteration texture and the most homogeneous texture.

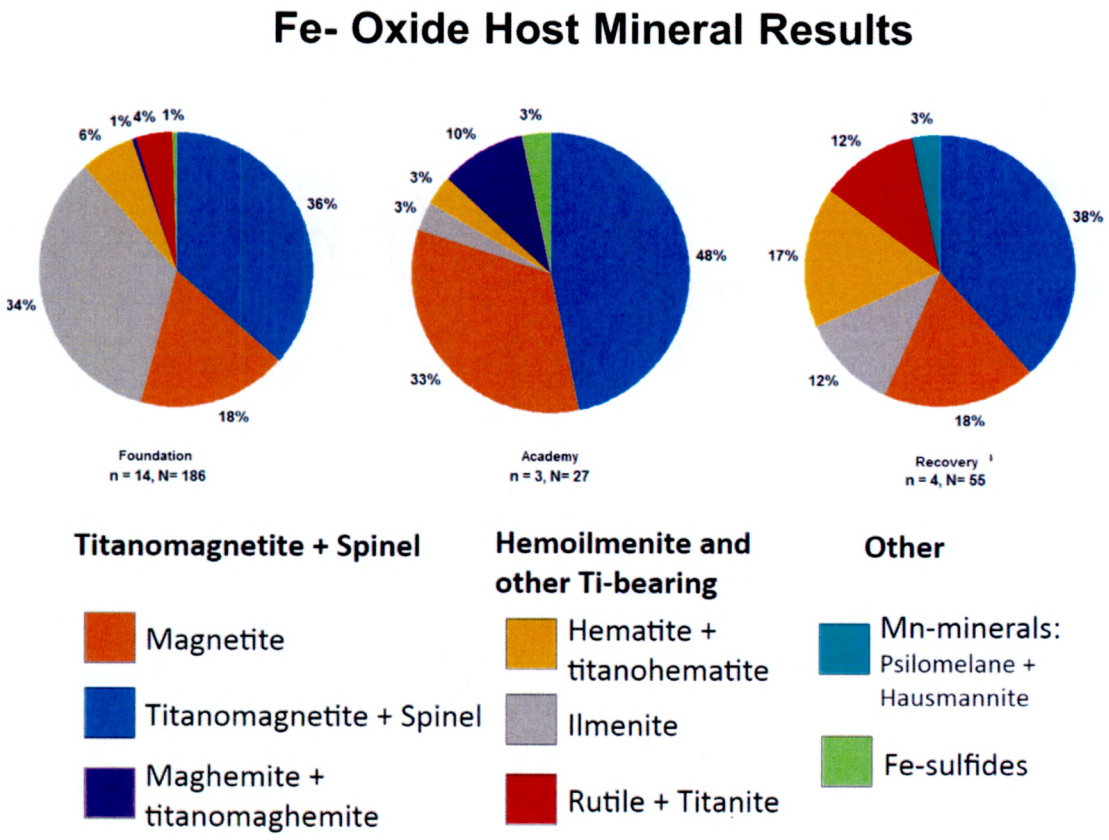

Figure 21. Comparison of Fe-oxide host mineral assemblages. The Foundation Ice Stream yields the most ilmenite. The Academy Glacier yields the most maghemite and the Recovery Ice Stream yields the only Mn- bearing minerals, including psilomelane and hausmannite.

Mn-bearing minerals such as psilomelane and hausmannite appear to be restricted to the Recovery Ice Stream, specifically within the southern margin till (WAW and WAW2). Recovery Ice Stream also has the least amount of Fe-oxide alteration textures and the highest amount of homogenous texture. This could indicate that there are more granitoids along Recovery Ice Stream's path. Brachfeld et al. (2013) observed Fe-oxide assemblages in Transantarctic Mountain basement units and in granitoids from the Granite Harbor Intrusive Complex, and observed homogeneous textures to be more common in granitoids. The Foundation Ice Stream contains the most ilmenite. The

Academy Glacier has the most alteration texture signifying that this ice stream, and its underlying bedrock, experienced the highest amounts of oxidation and/or hydrothermal alteration.

Micronutrients and redox-sensitive elements used for paleoclimate studies include, but are not limited to Fe, Mn, and V. As shown below (Fig. 22), the abundance of all three elements within each ice stream is comparable to the global average upper continental crust values determined by Taylor and McLennan (1985). This study did not measure what portion of the Fe in the fine fraction is bioavailable. However, observations of increased chlorophyll levels and phytoplankton abundance adjacent to large drifting icebergs in the Weddell Sea suggests that icebergs calved from the Ronne-Filchner system can stimulate productivity in the Weddell Sea (Smith et al., 2007; Duprat et al., 2016). The V and Mn results reported here suggest that redox signatures analyzed in Weddell Sea sediment cores will not be obscured by detrital interference.

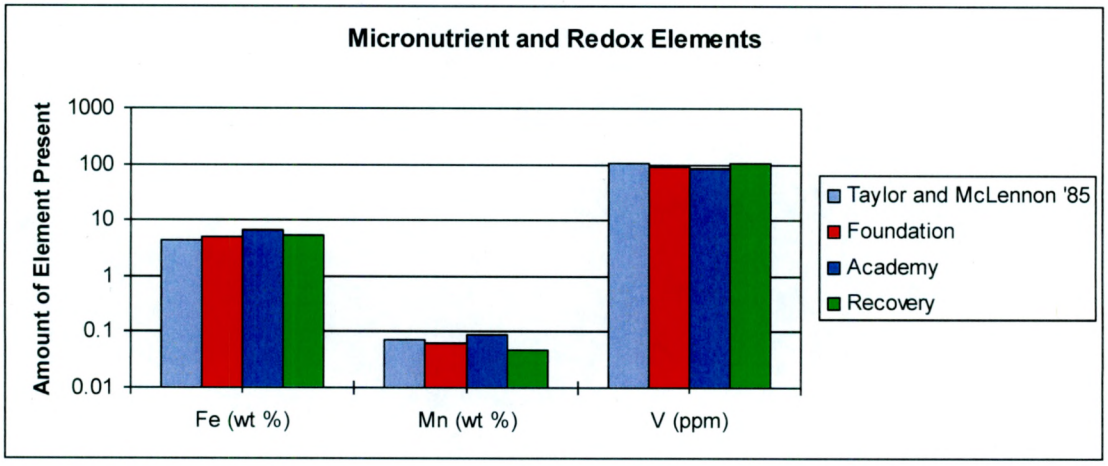

Figure 22. Comparison of micronutrient and redox element abundances (Fe, Mn, and V) between the global average upper continental crust of Taylor and McLennan, 1985, and the Foundation, Academy, and Recovery ice streams. All ice streams are comparable to the average upper continental crust.

Further review of the Fe-oxide EDS results indicates that magnetite and titanomagnetite found within all ice streams can be differentiated by the presence of specific impurities. The Academy Glacier has the least amount of impurities within magnetite, with only Al above detection via SEM-EDX. The Recovery Ice Stream contains Mn, Mg, Al, and Ca- bearing magnetite, while the Foundation Ice Stream is the only ice stream with V-bearing titanomagnetite.

Generating grain-by-grain Fe-oxide geochemical profiles to build an assemblage could be a way to match IRD in marine cores back to their most probable source, a method that has proven successful in the Arctic Ocean (Darby and Bischoff 1996, 2001). This combined with the ascertained mineral signatures of the three Weddell Sea sector ice streams could allow researchers to develop proxy records for ice stream activity in marine sedimentary records.

7. Conclusions

Through multiple petrological, geochemical, and geochronological analyses presented here and conducted by project collaborators, it can be concluded that these three ice streams within the Weddell Sea sector have observable differences between them. The geochemistry results presented here are consistent with the average upper continental crust materials in the drainage basins that house these ice streams. This is consistent with lithic clast observations made in the field, with the field team reporting abundant sandstones, quartzites, and metasedimentary units. Al/Ti and Fe/Ti ratio and CIA differences are also observed, but they are subtle and not suitable for fingerprinting for this project. All three ice streams contain average amounts of Fe, Mn, and V relative to global average upper continental crust.

A future project goal will include using trace element abundances in magnetite and titanomagnetite as a tracer of individual ice streams, with Al, V, Mn, Mg, and Ca having the greatest potential to distinguish between these three ice streams. In addition, principal component analysis (PCA) of the trace element data is pending as a means of exploring whether distinctive groups of trace elements occur in each ice stream.

Developing these geochemical and mineral signatures of three Weddell Sea sector ice streams (Foundation, Academy, and Recovery) allows researchers to develop proxy records for ice stream activity in marine sedimentary records. This also helps in better understanding records of ice sheet advance and retreat recorded in offshore sediment cores for this area as well as provide further insight as to which ice streams may be the most vulnerable to ice loss as a response to global warming.

8. References Cited

Agrios, L., Licht, K., Hemming, S.R., Williams, T., 2016. Using U-Pb Detrital Zircon Geochronology to Study Ice Streams in the Weddell Sea Embayment, Antarctica. Fall 2016 Meeting of the American Geophysical Union, San Francisco, CA.

Bamber, J.L., Alley, R.B., Joughin, I. 2007. Rapid response of modern day ice sheets to external forcing. Earth and Planetary Science Letters 257:1-13.

Biscaye, P.E. 1965. Mineralogy and Sedimentation of Recent Deep-Sea Clay in the Atlantic Ocean and Adjacent Seas and Oceans. Geological Society of America Bulletin 76:803-832.

Brachfeld, S., Pinzon, J., Darley, J., Sagnotti, L., Kuhn, G., Florindo, F., Wilson, G., Ohneiser, C., Monien, D., Joseph, L. 2013. Iron oxide tracers of ice sheet extent and sediment provenance in the ANDRILL AND-1B drill core, Ross Sea, Antarctica. Global and Planetary Change 110: 420-433.

Cirone, A., Brachfeld, S., Cortes, I., Verhagen, C., Williams, T., and Hemming, S., 2016. Provenance Tracing of Glacial Sediment from the Foundation, Academy, and Recovery Ice Streams, Weddell Sea, Antarctica. Fall 2016 Meeting of the American Geophysical Union, San Francisco, CA.

Craddock, C. Tectonic Map of Antarctica. 1970. American Geographical Society.

Darby, D.A. and Bischof, J.F. 1996. A statistical approach to source determination of lithic and Fe-oxide grains: An example from the Alpha Ridge, Arctic Ocean. Journal of Sedimentary Research 66:599–607.

Darby, D.A., Myers, W., Herman, S., Nicholson, B., 2015. Chemical Fingerprinting, A Precise and Efficient Method to Determine Sediment Sources. Journal of Sedimentary Research 85:247-253.

Duprat, L. P. A. M., Bigg, G.R., Wilton, D.J., 2016. Enhanced Southern Ocean marine productivity due to fertilization by giant icebergs, Nature Geoscience 9:219-221.

Farmer, G. L., K. Licht, R. J. Swope, and J. Andrews (2006), Isotopic constraints on the provenance of fine-grained sediment in LGM tills from the Ross Embayment, Antarctica, Earth and Planetary Science Letters 249(1-2):90-107.

Faure, G., Mensing, T.M., 2010. Shackleton Range and Theron Mountains. The Transantarctic Mountains: Rock, Ice, Meteorites, and Water. Dordrecht: Springer, 246-257.

Ford, A.B., 1976. Stratigraphy of the Layered Gabbroic Dufek Intrusion, Antarctica. Bulletin 1405-D.

Ford, A.B., Schmidt, D.L., Boyd, W.W., 1978. Geology of the Davis Valley Quadrangle and Part of the Cordiner Peaks Quadrangle, Pensacola Mountains, Antarctica. Department of the Interior. United States Geological Survey Report, 2-5.

Fretwell, P., Pritchard, H.D., Vaughan, D.G., Bamber, J.L., Barrand, N.E., Bell, R., Bianchi, C., Bingham, R.G., Blankenship, D.D., Casassa, G., Catania, G., Callens, D., Conway, H., Cook, A.J., Corr, H.F.J., Damaske, D., Damm, V., Ferraccioli, F., Forsberg, F., Fujita, S., Gim, Y., Gogineni, P., Griggs, J.A., Hindermarsh, R.C.A., Holmlund, P., Holt, J.W., Jacobel, R.W., Jenkins, A., Jokat, W., Jordan, T., King, E.C., Kohler, J., Krabill, W., Riger-Kusk, M., Langley, K.A., Leitchenkov, G., Leuschen, C., Luyendyk, B.P., Matsuoka, K., Mouginot, J., Nitsche, F.O., Nogi, Y., Nost, O.A., Popov, S.V., Rignot, E., Rippen, D.M., Rivera, A., Roberts, J., Ross, N., Siegert, M.J., Smith, A.M., Steinhage, D., Studinger, M., Sun, B., Tinto, B.K., Welch, B.C., Wilson, D., Young, D.A., Xiangbin, C., Zirizzotti, A., 2013. Bedmap2: Improved ice bed, surface and thickness datasets for Antarctica. The Cryosphere 7: 375-393.

Golledge, N.R., Levy, R.H., McKay, R.M., Naish, T.R., 2017. East Antarctic ice sheet most vulnerable to Weddell Sea warming. Geophysical Research Letters 44:2343-2351.

Haug, G.H., Hughen, K.A., Sigman, D.M., Peterson, L.C., Rohl, U., 2001. Southward Migration of the Intertropical Convergence Zone Through the Holocene. Science 239:1304-1307.

Hillenbrand, C-D., Bentley, M.J., Stolldorf, T.D., Hein, A.S., Kuhn, G., Graham, A.G.C., Fogwill, C.J., Kristofferson, Y., Smith, J.A., Anderson, J.B., Larter, R.D., Melles, M., Hodgson, D.A., Mulvaney, R., Sudgen, D.E., 2014. Reconstruction of changes in the Weddell Sea sector of the Antarctic Ice Sheet since the Last Glacial Maximum. Quaternary Science Reviews 100:111-136.

Košler, J., Fonneland, H., Sylvester, P., Tubrett, M., Pederson, R-B., 2002. U-Pb dating of detrital zircons for sediment provenance studies – a comparison of laser ablation ICPMS and SIMS techniques. Chemical Geology 182:605-618.

Latimer, J.C., Fillippelli, G.M., Hendy, I.L., Gleason, J.D., Blum, J.D., 2006. Glacial-Interglacial terrigenous provenance in the southeastern Atlantic Ocean: The importance of deepwater sources and surface currents. Geological Society of America 34:545-548.

Licht, K.J., Lederer, J.R., and Swope, R.J. 2005. Provenance of LGM Glacial Till (sand fraction) across the Ross Embayment, Antarctica. Quaternary Science Reviews 24:1499-1520.

Nesbitt H.W., Young, G.M. 1982. Early Proterozoic climates and plate motions inferred from major element chemistry of lutites. Nature 299:715-717.

Orsi, A. H., Johnson, G.C., and Bullister J.L., 1999. Circulation, mixing and production of Antarctic bottom water. Progress in Oceanography 43:55–109.

Passchier, S., 2007. Chapter 27, The Use of Heavy Minerals in the Reconstruction of Ice-Sheet Drainage Patterns: An Example from the Edge of the East Antarctic Ice Sheet. Developments in Sedimentology 58:677-699.

Pierce, E., Hemming, S.R., Williams, T., van de Flierdt, T., Thomson, S.N., Reiners, P.W., Gehrels, G.E., Brachfeld, S. A., Goldstein, S.L., 2014. A comparison of detrital U-Pb zircon, 40Ar/39Ar hornblende, and 40Ar/39Ar biotite ages in marine sediments off East Antarctica: implications for the geology of subglacial terrains and provenance studies, Earth Science Reviews 138:156–178.

Rignot, E., Mouginot, J., and Scheuchl, B., 2011. Ice Flow of the Antarctic Ice Sheet. Science 333(6048):1427-430.

Roy, M., van de Flierdt, T., Hemming, S., Goldstein, R., 2007. 40Ar/39Ar ages of hornblende grains and bulk Sm/Nd isotopes of circum-Antarctic glacio-marine sediments: Implications for sediment provenance in the southern ocean. Chemical Geology 244:507–519.

Schmidt, D.L., Ford, A.B., 1969. Geology of the Pensacola and Thiel Mountains. Geologic Map of Antarctica. American Geographical Society. Sheet 5.

Smith, K.L., Robison, B.H., Helly, J.J., Kaufman, R.S., Ruhl, H.A., Shaw, T.J., Twining, B.S., and Vernet, M., 2007. Free-Drifting Icebergs: Hot Spots of Chemical and Biological Enrichment in the Weddell Sea. Science 317 (5837):478-482.

Stewart, J., 2011. Antarctica: An encyclopedia, 2nd Edition, Volumes 1 and 2. McFarland and Company, Inc., Jefferson, North Carolina, and London.

Suk, D., Peacor, D.R., Van der Voo, R., 1990. Replacement of pyrite framboids by magnetite in limestone and implications for paleomagnetism. Nature 345:611-613.

Taylor, S.R., McLennan, S.M. 1985. The Continental Crust: Its Composition and Evolution. Blackwell Scientific Publication, Carlton, 312.

Thoma, M., Determann, J., Grosfeld, K., Goeller, S., Hellmer, H. 2015. Future sea-level rise due to projected ocean warming beneath the Filchner Ronne Ice Shelf: A coupled model study. Earth and Planetary Science Letters 431:217-224.

Williams, T., van de Flierdt, T., Hemming, S.R., Chung, E., Roy, M., and Goldstein, S.L., 2010. Evidence for iceberg armadas from East Antarctica in the Southern Ocean during the late Miocene and early Pliocene, Earth and Planetary Science Letters 290:351–361.

Williams, T, Licht, K, Hemming, S, Kuhn, G, van de Flierdt, T, Brachfeld, S, Torfstien, A, Hillenbrand, CD, Flowerdew, M, Braddock, P., 2015. Ice dynamics in the Weddell Sea embayment of Antarctica using sediment provenance. AGU Joint Assembly, Montreal, Canada, 3-7 May 2015.

Williams, T., Hemming, S. R., Boswell, S., Licht, K., Brachfeld, S.A., Flierdt, T., Kuhn, G., Hillenbrand, C.D., Zhai, X. 2016. Using Sediment Provenance to Study Ice Streams in the Weddell Sea Embayment of Antarctica. Fall Meeting, AGU, San Francisco, CA, 12-16 December, 2016.

Yarincik, K.M., Murray, R.W., 2000. Climatically sensitive eolian and hemipelagic deposition in the Cariaco Basin, Venezuela, over the past 578,000 years: Results from Al/Ti and K/Al. Paleoceanography 15:210-228.